How Epstein Barr Virus Amplifies its Genome Productively

By

Thejaswi Nagaraju

A dissertation submitted in partial fulfillment of the requirements for the degree of

Doctor of Philosophy
(Physiology Graduate Training Program)

at the University of Wisconsin-Madison
2020

Date of final oral examination: 11/20/2020

The dissertation is approved by the following members of the Final Oral Committee:
Bill Sugden, Professor, McArdle Laboratory for Cancer Research
Beth Weaver, Associate Professor, McArdle Laboratory for Cancer Research
Nate Sherer, Associate Professor, McArdle Laboratory for Cancer Research
Norman Drinkwater, Professor, McArdle Laboratory for Cancer Research
Paul Ahlquist, Professor, McArdle Laboratory for Cancer Research

Table of Contents

Acknowledgements

I have had the chance to surround myself with some outstanding individuals over the course of the last years in Madison. These individuals have shaped me in becoming not only a better scientist but also a better person.

To Donata Oertel- I would like to dedicate my dissertation to Donata Oertel. Donata was the chairman of the physiology graduate training program. Donata was one of the most dedicated, caring and cheerful human being I have met in my life. She went above and beyond to help me overcome my adversities. She was the sole reason I was initially able to start my graduate education in Madison.

To Bill Sugden: Thank you for mentoring me throughout my graduate education, not just in science but in all aspects of my life. Your mentoring has not only made me a better scientist but also a better human being. You have been my role model and will continue to be my role model for the rest of my llife.

To my committee members, Beth Weaver, Kate O'Connor-Giles, Nathan Sherer, Norman Drinkwater, and Paul Ahlquist: Thank you for lifting my spirits during times in graduate career when not everything worked smoothly. I also thank you for all the terrific scientific discussions during committee meetings. It truly made a difference to my scientific thinking.

To the past and current lab members of the Sugden Lab, Ya-Fang Chiu, Ngan Lam, Yachun Yang, Asuka Nanbo, Celia Bisbach, Aurelia Faure, Danielle Westhoff Smith, Adityarup Chakravorty, Mitchell Hayes, Quincy Rosemarie and Rebecca

Hutcheson- Thank you for being such terrific colleagues. My stay in the lab was delightful largely due to your presence. Your insights in science and beyond has helped me shaped my thinking over the years.

To all my friends in Madison: Thank you for making my stay in Madison wonderful. I would like to thank Akshay Sood, Becky Callan, Ellen Sjolund, Kai Russo, Matt Gawlik and Laurel Legenza for having me as a part of your group. It truly has been a pleasure knowing you guys. Pankaj Dubey, William Dean and Gregorio Rodriguez- Thank you for being such wonderful and welcoming roommates. I enjoyed all those long discussions with you and all the times we spent time together.

To Mehrdad Arjmand- Thank you for being such a wonderful friend. I felt I grew everytime I spoke to you. I have enjoyed your friendship so far and I look forward to a lifetime of friendship

To my partner, Anne Manero Alvarez- Thank you for being there for me during the tough times! Thank you so much helping me become a better person and always keeping me honest. I look forward to all our adventures in the future. I also look forward to growing together with you.

To my mother, GR Savithri- Thank you for ALWAYS being there for me. I couldn't have been here without your unconditional support and love on good and bad days. Despite being thousands of miles away, I appreciate your support. You were, are and always will be a constant source of motivation for me.

List of Figures and Tables

List of abbreviations

Abbreviation	Full Name
ACE 2	Angiotensin-Converting Enzyme 2
ARF	Auxin Response Factor
Au	Auxin
BAC	Bacterial Artificial Chromosome
BSA	Bovine Serum Albumin
BALF2	BamHI A Leftward Fragment 2
BALF5	BamHI A Leftward Fragment 5
BBLF4	BamHI B Leftward Fragment 4
BBLF2/3	BamHI B Leftward Fragment 2/3
BBRF1	BamHI B Rightward Fragment 1
BHLF1	BamHI H Leftward Fragment 1
BHRF1	BamHI H Rightward Fragment 1
BMLF1	BamHI M Leftward Fragment 1
BRLF1	BamHI R Leftward Fragment 1
BSLF1	BamHI S Leftward Fragment 1
BZLF1	BamHI Z Leftward Fragment 1
BcLF1	BamHI c Leftward Fragment 1
Bp	Basepair
BrdU	BromodeoxyUridine
CMV	Cytomegalovirus
DMEM	Dulbecco's Modified Eagle Medium
DAPI	4′,6-diamidino-2-phenylindole
DNA	Deoxyribonucleic Acid
Dox	Doxycycline
EBNA1	Epstein Barr Nuclear Antigen 1

EBV	Epstein Barr Virus
EdC	5-Ethynyl-2'-deoxycytidine
EdU	5-Ethynyl-2´-deoxyuridine
EDTA	Ethylenediaminetetraacetic Acid
ERGIC	Endoplasmic Reticulum-Golgi Intermediate Complex
FBS	Fetal Bovine Serum
FISH	Fluorescent In Situ Hybridisation
GFP	Green Fluorescent Protein
HA	Hemagglutinin
HEPES	4-(2-hydroxyethyl)-1-piperazineethanesulfonic Acid
HH	Heavy Heavy
HL	Heavy Light
HEK 293	Human Embryonic Kidney 293
HSV1	Herpes Simplex Virus 1
IAA	Indole-3-Acetic Acid
IE	Immediate Early
KSHV	Kaposi Sarcoma associated Herpesvirus
MLS	Mitochondrial Localization Sequence
mSc	monomeric Scarlett
NCI	National Cancer Institute
NCBI	National Center for Biotechnology Information
NES	Nuclear Export Signal
NLS	Nuclear Localization Sequence
nt	nucleotide
O	Origin
ORF	Open Reading Frame
OsTIR1	Oryza sativa Transport Inhibitor Response 1
PBS	Phosphate Buffer Saline

PEL	Primary Effusion Lymphoma
SARS-CoV-2	Severe Acute Respiratory Syndrome Coronavirus 2
STED	Stimulated Emission Depletion
STORM	Stochastic Optical Reconstruction Microscopy
TMPRSS2	Transmembrane Protease, Serine 2
TE	Tris EDTA
TR	Terminal Repeats
TRS	Transcriptional Regulatory Sequence
UTR	Untranslated Region
Z	BamHI Z Leftward Fragment 1
ZRE	Z Response Element

CHAPTER 1. INTRODUCTION

Herpesviruses are a family of DNA viruses that cause diseases in many different animals including humans [1]. Based on their DNA sequences, herpesviruses are broadly classified into three subfamilies: α-herpesviruses, β-herpesviruses, and γ-herpesviruses. All herpesviruses display two phases in their life-cycle – the latent phase and the lytic phase. During the latent phase, the viruses reside in the nucleus of the host as plasmids with minimal viral gene expression. Viral plasmid synthesis is mediated by cellular machinery in a licensed manner. In contrast, during the lytic phase of their life cycle, herpesviruses amplify their genomes to high levels. This DNA synthesis, which leads to DNA amplification during the lytic phase, is unlicensed and is mediated by viral replication machinery. Our understanding of viral DNA amplification of herpesviruses is rudimentary. Here I will introduce several aspects of Epstein Barr Virus (EBV) and Kaposi Sarcoma Associated Herpesvirus (KSHV)(γ-herpesviruses) DNA amplification. These aspects include roles of the origin of lytic DNA replication and replication compartments in DNA amplification. I will also compare different facets of DNA amplification in both γ-herpesviruses and other herpesvirus subgroups.

γ-herpesviral DNA amplification:

γ-herpesviruses, including EBV and KSHV, cause several human cancers such as Burkitt's lymphoma, nasopharyngeal carcinoma and primary effusion lymphoma (PEL). Collectively they account for about 300,000 new cases each year. EBV and

KSHV initially infect cells latently with few exceptions; that is, an initial infection does not result in the production of progeny virus [2]. For EBV, once a latent infection is established, the cells rarely support a switch to a productive infection. For example, 1 in 10^3 to 1 in 10^6 B cells latently infected with EBV supports the lytic cycle per 24 hours to yield the virus necessary for the spread of infection [3,4]. This rare event supports both synthesis of progeny virus and results in the lysis of infected cells.

During the lytic phase, γ-herpesviruses amplify their DNA approximately 1000-fold within 12-13 hours in individual cells [5–7], as do the α- and β-herpesviruses as exemplified by Herpes Simplex Virus-1 (HSV-1) and human Cytomegalovirus (HCMV) [5–7] respectively. This amplification follows the arrest of the host cell cycle at the beginning of S-phase such that no cellular DNA synthesis subsequently occurs [7,8]. These findings indicate that herpesviruses likely divert the resources meant for cellular DNA replication toward viral DNA amplification. This subversion is also common among other herpesviruses including α- and β-herpesviruses. For EBV, entry into the lytic phase is triggered by the expression of its immediate-early (IE) genes, BamHI R Left Fragment 1(BRLF1, termed R here onwards), and BamHI Z Left Fragment 1(BZLF1, termed Z here onwards) and for KSHV, by its IE gene, Rta. These genes encode transcription factors that mediate the transcription of the viral early genes required for viral DNA replication. The newly replicated DNA molecules serve as templates for late gene transcription and as genomes to be encapsidated into new viral particles [9]. This viral DNA synthesis and subsequent transcription is mediated within viral replication compartments which are initiated at the start of the lytic phase after the subversion of the cell cycle machinery.

Given that the unfolding of the lytic phase is cell-cycle dependent, studying its different facets – such as DNA amplification – poses a technical difficulty because cells in an asynchronous population differ in their stages of the cell cycle and consequently, their stages of the lytic phase at any given time. The problem is exacerbated in the case of γ-herpesviruses, because at any time, only a small fraction of infected cells enters the lytic phase.

I will focus on several facets of herpesvirus DNA amplification during the lytic phase, including the viral origin of DNA replication, the structure of the viral DNA, and the role of replication compartments in DNA amplification by way of introduction to my own research.

Role of the viral origin in γ-herpesviral DNA amplification

Herpesviruses use different origins of replication in their latent and lytic phase. During the lytic phase, EBV and KSHV use their respective oriLyts [10,11], which act in *cis.* This DNA element contains the genetic information required to initiate synthesis of viral genomes and may be required for continuous DNA replication after initiation. OriLyt underlies the viruses' ability to initiate DNA synthesis and consequently amplify their DNA. Its essential features include: 1) Sites that contribute mechanistically to viral DNA amplification, and 2) Sites that interact with *trans*-elements to execute initiation of DNA amplification. Derivatives of EBV and KSHV lacking their respective oriLyts were shown to be defective for viral DNA amplification during the lytic phase [9,11]. OriLyt in EBV was identified by restriction mapping and functional analysis of the EBV genome. Unique fragments from EBV (inserted in a plasmid) were transfected into Burkitt's lymphoma cells and subsequently, the lytic phase was induced. Fragments that triggered

replication of the respective plasmids were identified as the origin, oriLyt. EBV's wild type OriLyt is 7.7 kb, and optimal amplification of EBV DNA during the lytic phase requires two such origins in the same genome [8,10]. The KSHV origin of lytic replication was identified using K8, the origin binding protein of KSHV. Based on its sequence, K8 was identified as an analog of EBV BZLF1. To identify KSHV's lytic origin, the KSHV genome was isolated and digested with restriction enzymes, and the fragments ligated to an adapter sequence to allow amplification of the fragments. These fragments were incubated with cell extracts obtained from the KSHV-positive cell line (BCBL-1) in which the lytic phase was induced. K8 was precipitated using an anti-K8 antibody and DNA bound to K8 was sequenced. Subsequently, two stretches of DNA with identical sequences that spanned 1.7kb were identified as KSHV oriLyt. These sequences are sufficient for viral DNA replication during KSHV's lytic phase [12]. However, extensive studies of the KSHV oriLyt haven't been carried out (in contrast to studies on EBV oriLyt, where stepwise mutational analyses have been carried out to understand the levels of DNA replication with differing portions of the oriLyt) to explain if 1.7kb oriLyt provides the same level of viral DNA replication efficiency as does its longer counterpart. The activation of the γ-herpesvirus oriLyt is mediated by the respective origin DNA binding proteins, BZLF1, and K8. In EBV, oriLyt has two components – an upstream component and a downstream component (Fig 1.1). The upstream component of the EBV oriLyt is also part of the promoter region of the BHLF1 gene. The downstream element is upstream of the BHRF1 gene. There are seven binding sites for Z within EBV's oriLyt and these sites are known as Z Responsive Elements (ZREs) [13,14]. Two of the ZREs (ZRE1-2) are within the upstream component, two in between the

upstream component and the downstream component, and three are in between the downstream component and BHRF1 gene[13] (Figure 1). Two lines of evidence indicate that the transcriptional activity of BZLF1 when it binds to ZRE1 and ZRE2 is required for DNA amplification from oriLyt. First, knocking out ZRE1 and ZRE2 reduces oriLyt's ability to activate lytic amplification to 20% of the wild type oriLyt's ability. Second, the motif within BZLF1 which is required for its transcriptional activity is also required for its ability to activate DNA replication [13]. Subsequently, it has been concluded that the RNA-DNA hybrid formed as a result of BHLF1 transcription is required for viral DNA replication, perhaps because RNA-DNA hybrid formation provides a template for the ssDNA binding protein BALF2, which is a core protein of the EBV replisome and is required for the replisome to bind to viral DNA[15]. To determine whether RNA-DNA hybrids are required for DNA replication, cells were transfected with RNaseH, which degrades RNA only when it is present as an RNA-DNA hybrid[15]. Indeed, the depletion of RNA-DNA hybrids at the oriLyt region correlated with reduced DNA synthesis. However, such experiments, while potentially informative, can be challenging to interpret due to the non-specific effects (cleavage of RNAs at sites other than oriLyt) RNaseH can have on the cells. KSHV, just like EBV, also has its oriLyt located at a region of its genome that consists of divergent promoters [16]. HSV1 and CMV also display similarities along the following lines: i) A transcriptional start site located in the intra-origin region, ii) The presence of persistent RNA-DNA hybrids at the lytic origin of replication, [17–20] based on experiments similar to those described above for EBV. These observations indicate that herpesviruses have evolved to couple origin activation with active transcription at the start of the lytic phase, and that this coupling is essential for a

successful lytic phase. Intriguingly, EBV plasmids lacking any detectable transcriptional activity around oriLyt also effectively support DNA replication to the same levels as wild type EBV[8]. Put together, EBV's oriLyt encodes multiple BZLF1 binding sites, which are initially required for viral DNA replication. However, two things are not clear- 1)The role of transcription in the initiation of DNA synthesis, and 2)The role of RNA-DNA hybrids in initiating DNA synthesis. Therefore, it is desirable to further our understanding to learn how oriLyt is primed for initiating DNA synthesis throughout the lytic phase.

Different herpesviruses usually contain two origins of DNA synthesis. Most strains of EBV harbor two copies of oriLyt, as do KSHV and murine γ-herpesvirus 68 (MHV 68). HSV1 harbors two origins as well: oriL and oriS [21], while CMV harbors only one oriLyt. C57BL/6 mice infected intranasally with MHV 68 harboring two lytic origins displayed greater viral titers in the lungs than mice infected with MHV68 harboring a single copy of its oriLyt [22]. Another study showed that EBV harboring two copies of oriLyt makes approximately 8 times more DNA during the lytic phase compared to EBV harboring one oriLyt[8]. This finding is consistent with the virus needing two copies of oriLyt to make more DNA, which could determine the number of viral particles produced. Combined, these findings indicate that several herpesviruses have been evolutionarily selected to harbor two copies of oriLyt to provide an advantage to these viruses during the lytic phase.

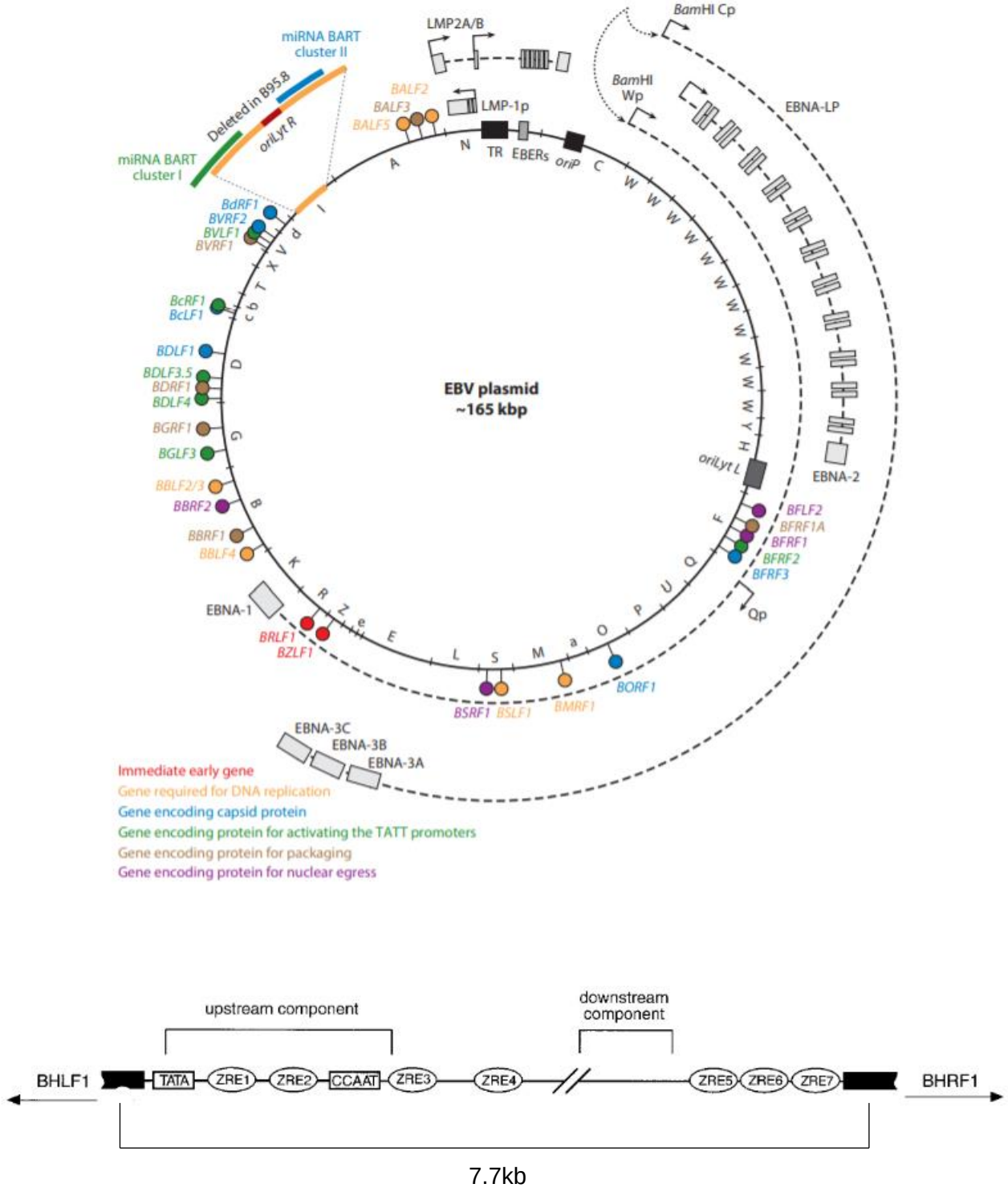

Figure 1.1: **Defining features of EBV and its oriLyt**- oriLyt spans 7.7 kb in length. ZRE1-7 are BZLF1 binding sites on oriLyt. The figure at the top has been adopted from [23] and the figure at the bottom has been adapted from [13]

Structure of viral DNA during the lytic phase

The structure of the replicating viral DNA (for example- theta replicon, rolling circle replicon, etc) during the lytic phase directly determines the kinetics of viral DNA synthesis. For example, bidirectional replication would have different kinetics compared to unidirectional DNA synthesis. Much of our understanding of the structure of viral DNA during the lytic phase comes from studies on HSV1, largely due to the efficiency with which HSV1 supports lytic infection in a wide variety of non-neuronal cell lines, unlike EBV and KSHV, which exist latently in multiple different cell types. The HSV1 DNA which is released as a linear genome in cells is first circularized, followed by the generation of longer-than-unit-length concatamers [24]. HSV1 DNA isolated from cells and analyzed by EM shows multiple species existing within the pool of isolated viral DNA including: i) circular DNA, ii) DNA with lariat structures consisting of linear segments longer than the unit length of the genome and a ring-like DNA attached to it, iii) linear DNA with internal gaps and segments of single-stranded DNA, and iv) a large tangled mass of DNA [25]. These findings indicate that the replication of viral DNA is unlikely to proceed via a single mechanism but instead proceeds via multiple mechanisms. All the observations of DNA made in this study were from a single time point (20hrs after HSV-1 infection) and therefore, the replicating viral DNA may also adopt different structures at earlier or later timepoints after HSV-1 infection. After the study mentioned above, others have shown the presence of viral DNA longer than the unit-length of a defective viral genome itself. They made this observation when they co-infected wt HSV-1 along with defective HSV-1 (this defective HSV-1 only contains *cis* elements but not the *trans* elements required for viral DNA replication) and smaller versions of HSV-1 genomes [26].

The lengths of both wild type and defective HSV-1 genomes were heterogenous and longer than unit length (upto 10-20 times longer than unit length for the defective HSV-1). The presence of longer than unit-length HSV-1 genomes indicated that at least at 20 hpi (the time at which the DNA was isolated), DNA synthesis is likely to proceed in a mechanism that is distinct from a canonical theta replication which does not entail changes in the length of replicating DNA. However, none of the studies compared the kinetics of DNA amplification (which is 500-1000-fold in approximately 12 hours) to the structure of the DNA. A simple rolling circle replication, as observed in T4 bacteriophage [27], which is also proposed for herpesviruses [28], is unlikely to explain a 500-1000-fold DNA amplification in a short duration. This amount of DNA amplification within 12 hours would require DNA synthesis with kinetics that resembles exponential DNA amplification. However, a pure rolling circle replication does not yield exponential DNA synthesis but instead is linear.

γ-herpesviruses such as EBV and KSHV begin the lytic phase as circular plasmids, but by the end of the lytic phase they are linear molecules. At the beginning of DNA replication, EBV DNA replication has been suggested to proceed via theta replication on the basis of experiments such as 2D-gel electrophoresis and CsCl-propidium iodide density gradients [29]. These experiments show the presence of replicated, open circular DNA characteristic of theta replication and an absence of linear DNA early during the lytic phase characteristic of rolling circle replication. A caveat to these studies is that they were carried out with asynchronous population of cells, limiting the ability to quantify the DNA synthesized. After the early stages of DNA replication,

DNA molecules appear to be concatemers, as evidenced by southern blots which show the presence of viral DNA molecules longer than the unit length of EBV[29] [30].

Recombination may play a role in modifying DNA structures during replication. Branched DNA structures have been observed during HSV1 replication, using pulse field electrophoresis [31]. These branched DNA structures likely arise from the rampant recombination events that are frequent during HSV1 DNA replication[21]. Some studies suggest that a single-stranded annealing mechanism is the primary mode of recombination during the lytic infection [32,33] while others suggest that homologous recombination occurs with high frequency. However, the mode of recombination that the virus adopts is still largely unclear.

To summarize, herpesviral DNA amplification during the early lytic phase likely proceeds via theta replication. However, it is not clear what is the mode(s) of DNA synthesis after the early stages of the lytic phase. It is also not clear how recombination enables viral DNA replication. Therefore, it would be desirable to analyze this DNA replication in depth after early stages of the lytic phase.

Replication Compartments- Beginning of the End

Replication compartments are sites of viral DNA synthesis that are formed at the very beginning of the herpesviral lytic phase in the nucleus of a cell [34]. Replication compartments have several key features: 1) They are completely devoid of any chromosomal DNA; 2) They lack any detectable canonical histones[7]; and 3) They grow over time in proportion to the DNA amplified within them.

Replication compartments are complex features of the lytic phase and several factors contribute to their formation. The products of immediate early genes and the early genes are required for the formation of replication compartments [35]. While cellular factors are almost certainly required as well, none have been reported. A key difference between EBV and HSV-1 at the start of the lytic phase is that EBV enters the lytic phase after being maintained latently in the cell while HSV-1 adopts this phenotype within hours after initial infection [21,29]. In the case of HSV-1, only about 7-8 molecules of the incoming HSV-1 DNA support the DNA amplification process [36]. In the case of EBV and KSHV, it is not clear if all the viral DNA molecules present latently begin to support the lytic phase. For EBV and HSV-1, replication compartments are clonal i.e., each compartment is initiated by a single viral genome [8,37]. While these compartments are initiated by single viral genomes, it is not clear if replication compartments are formed at predetermined sites within the nucleus. For KSHV, it is not clear if single genomes initiate replication compartments. However, KSHV biology provides a few interesting possibilities. KSHV clusters its plasmids frequently during its latent phase. Clustering here refers to several plasmids (>2) collectively present at the same locus. Therefore, it is not clear if the findings from HSV-1 and EBV that replication compartments are clonal can be extrapolated to KSHV. One possibility is that only one molecule within a cluster gives rise to a replication compartment. The second possibility is that several plasmids within the cluster give rise to replication compartments. The third possibility is that a cluster of plasmids does not give rise to a replication compartment but instead plasmids which are present individually as opposed to a cluster gives rise to a replication compartment. The above scenarios are not mutually exclusive, therefore all the

scenarios might simultaneously occur in a population of cells that support KSHV's lytic phase. A microscopic analysis of KSHV's switch from the latent to the lytic phase is likely to yield interesting results because KSHV is the only herpesvirus so far which shows the phenotype of clustering during the latent phase [38].

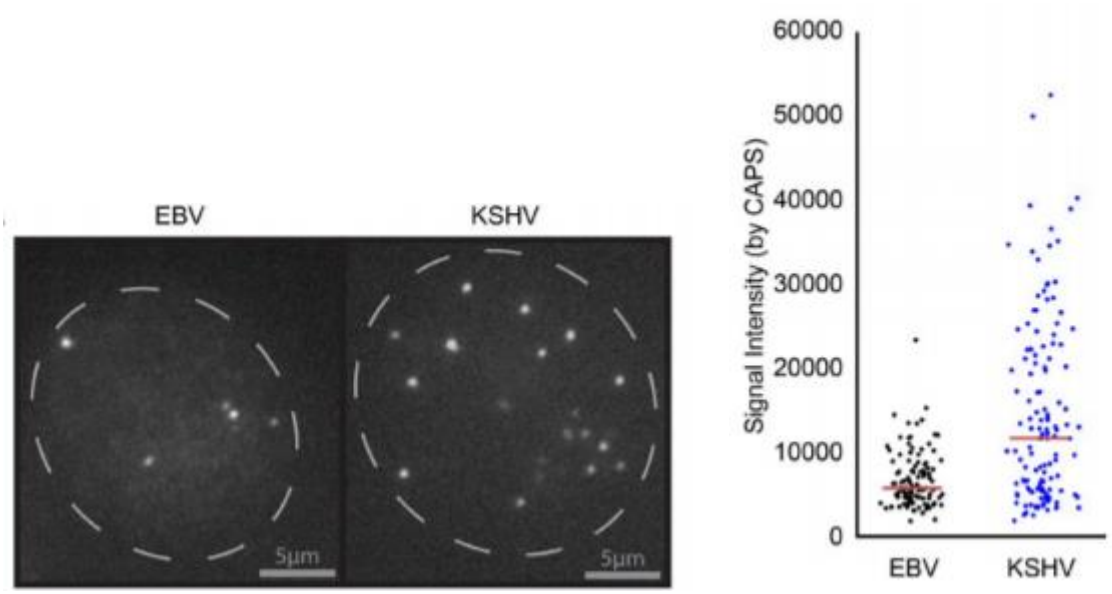

Figure 1.2 EBV and KSHV plasmids prior to the lytic phase- EBV plasmids exist individually in the nucleus while KSHV plasmids cluster as indicated by intense signals. The figure was adopted from [38]. EBV was analyzed in BC-2 cells and KSHV was analyzed in BCBL-1 cells using FISH.

As DNA amplification proceeds, replication compartments grow in volume and eventually coalesce with adjacent compartments. This coalescence, in the case of HSV-1, has been shown to facilitate the export of mRNA[39]. The consequences of the coalescence of γ-herpesviral replication compartments are not understood. Replication compartments grow concurrently with increased DNA amplification and eventually

occupy up to 30% of the nuclear volume. A 1000-fold DNA amplification means that the viral DNA makes up ~30% of the total DNA present in the nucleus. One study shows that replication compartments continue to exist during the lytic phase, if and only if there is continuous viral DNA synthesis, indicating that there is a tight link between replication compartments and DNA amplification within them [40]. However, a caveat in the study is that replication compartments are visualized using BMRF-1-GFP (BMRF-1 is a processivity factor for viral DNA amplification) instead of visualizing the viral DNA directly. One artifact of this study could be that inhibition of DNA amplification might lead to a redistribution of viral replication proteins but maintain replication compartments containing the viral DNA.

Throughout the lytic phase, different factors limit the process of DNA amplification. At the start of DNA amplification, the number of DNA templates limits the amount of DNA amplification. Throughout the lytic phase, the ratio of early gene products (with the BMRF-1 gene product serving as a surrogate for early gene products) and DNA molecules drastically decreases, likely making early gene products candidates for limiting factors later during the lytic phase [8]. This reduction in early gene products is likely to result from host shut-off proteins, BGLF5 for EBV and SOX for KSHV, degrade mRNA of early genes [41,42] leading to a reduced stoichiometry of replicative proteins for every DNA template present. Additionally, several cellular factors likely aiding viral DNA replication also might be limiting due to the degradation of host mRNAs by the host shut-off proteins. To summarize, the replication compartments coordinate viral DNA synthesis in a rapidly evolving environment, providing the genomes with which to generate viral particles. Therefore, it is desirable to understand

the role of replication compartments in aiding DNA replication such that adequate amplification is achieved successfully.

To summarize, there are several gaps in knowledge associated with our understanding of DNA amplification of herpesviruses. In our studies, we have examined several factors that contribute to DNA amplification of EBV. We study EBV of all the herpesviruses because it provides a model in which the transitioning from the latent to lytic phase is facile.

We have assessed the role of multiple oriLyts in DNA amplification and have found that the total level of viral DNA amplified is proportional to the number of oriLyts in individual genomes. The rate at which single DNA molecules are synthesized is proportionally higher in molecules with two oriLyts compared to molecules with only one oriLyt.

The number of viral genomes at the beginning of the lytic phase contributes to the levels of viral DNA amplified. These individual viral genomes seeded individual replication compartments which supported similar levels of viral DNA syntheses indicating that replication compartments indeed regulate the levels of viral DNA synthesis. Surprisingly, of all the viral DNA that was amplified, only ~1% of it was successfully packaged into viral particles.

The replication compartments which support viral DNA synthesis, took 12-13hrs to reach their maximum volume which was approximately 30% of the nuclear volume. During this process, some of the viral proteins such as BMRF-1 which were initially in

excess became limiting in concentration at the later stages of the lytic phase, potentially restricting the levels of DNA synthesis.

CHAPTER 2.

MATERIALS & METHODS

Quantitative PCR

Probes were labeled with 5'-FAMRA and 3'-TAMRA (IDT, Integrated DNA Technologies, Coralville, IA). For detection of EBV DNA, 4uL of purified total DNA per reaction was used as template, with primers and probe specific for the BALF5 sequence (as an internal control, cellular DNA was also detected using primers and probe specific to rhodopsin). The reactions were incubated at 50°C for 2 minutes, then at 95°C for 10 minutes followed by 40 cycles of 95°C for 15 seconds and 60°C for 1 minute. Data were collected on a 7900HT real-time instrument (Applied Biosystems) and analyzed using SDS Version 2.2.2 or 2.2.4 software. Fold changes were based on the assumption that amplicon levels increase by 1.8 times every cycle. Linearized plasmids were used for standard controls [43]

Live-Cell Imaging

A Leica TCS-SP8 laser scanning confocal microscope was used to follow live cells maintained in a Tokei-Hit Bio chamber at 37C, 5% CO_2 for approximately 40 hours. Cells were imaged every 90 minutes and sixty to seventy z-slices were captured with 0.35 µm between each successive z-plane. Images were subsequently processed using ImageJ.

EdU-pulse labeling

Cells were pulsed with EdU at a final concentration of 10uM for various amounts of time depending on the experiment. The cells were washed with PBS and fixed with 4% paraformaldehyde (PFA) in PBS for 10 minutes, washed with PBS, and

permeablized with 0.2-0.5% TritonX-100 for 15minutes. Cells were washed after permeablization and incubated with a labelling cocktail (copper sulphate, ascorbic acid and Cy5 azide) as described in [44] for 30 min. Cells were washed with PBS and mounted on to coverslip with media containing DAPI.

EdU-pulse labelling and Immunofluorescence

Cells pulsed with 10uM final concentration of EdU were washed and fixed with 4% Paraformaldehyde (PFA) in PBS for 10 minutes, washed with PBS, and permeablized with 0.2-0.5% TritonX-100 for 15minutes. EdU was used as described above in the previous method. The cells were incubated with PBS+2% BSA for two hours and labelled with a primary antibody in 2% BSA (anti BMRF1 at 1:3000 or anti-HA at 1:2000) for two hours. The cells were washed three times with PBS+2% BSA and incubated with a secondary antibody (fluorescent dye-conjugated at 1:1000) for two hours. The cells were washed three times with 2% BSA and mounted with mounting media containing 2ug/mL DAPI.

Density-shift experiment

Approximately $5x10^6$-$1x10^7$ cells were plated on 15cm dishes and allowed to adhere to the surface (approx. 16-18hrs). The cells were induced with 200nM Tamoxifen for 8-10 hours. 100uM of BrdU and 200uM deoxycytidine were added for either 30, 60,90,120, 180 min. The cells were washed with ice-cold PBS, trypsinized, pelleted, resuspended in 1mL PBS, and sonicated three times with 10s on, 30s off cycle at an amplitude of 2 (Ultrasonic Processor; Model CV18). The DNA was purified by

phenol-chloroform extraction followed by ethanol precipitation and resuspended in 500uL of 10mM Tris,1mM EDTA. The DNA was sheared by passing through a 26 gauge (½ inch) needle 6-9 times. 10-20ug of DNA from each sample were mixed with 9.4mL of CsCl chloride solution reaching a final refractive index between 1.4002-1.402 in a Beckmann Coulter 5/8X3 in centrifuge tube. The tubes were spun at 40,000rpm at 23°C in an 80Ti rotor for approximately 63hrs,and fractionated into 250uL fractions. 100uL from each fraction was dialyzed using drop dialysis (two times) on a membrane (0.025um VSWP filter type from Millipore) for 1hr each time. 4uL from each DNA fraction were assayed for the amounts of viral DNA (probe against BALF5) and cellular DNA (probe against rhodopsin) using qPCR (ABI7900). Input DNA was measured for viral and cellular DNAs using qPCR to monitor their recovery.

Analysis of extracellular viral particles

1.2mL of cell supernatants were collected and clarified by centrifugation at 12000rpm for 5min to remove the cellular debris. 1mL was carefully collected and treated with 10ug of DNAse in the presence of 2mM $MgCl_2$ at 37°C for 30 min. A final concentration of 4mM of EDTA was added to quench the reaction. The sample was treated with Proteinase K at a final concentration of 100ug/mL for 2hr at 56°C. The DNA was purified by phenol-chloroform extraction followed by ethanol precipitation and quantified using quantitative PCR.

Analysis of intracellular capsids

1-2X10^6 cells were harvested and lysed by sonication (Ultrasonic Processor;Model CV18;10s on, 30s off at an amplitude of 2) for 3-5 cycles in PBS. The supernatant was clarified by spinning at 2000 rpm for 10 min in an Allegra X-15R centrifuge in a swinging bucket rotor and layered onto a 20% sucrose cushion and spun at 24000 rpm in SW50.1 rotor for one hour [45] . The supernatant was carefully removed and the pellet was resuspended in TE (Tris 10mM-EDTA 1mM) for 2hrs and processed just as was done for analysis of extracellular capsids above.

Generation of HEK 293 cells containing EBV mutants

EBV bacmids MI-197 (Δ BcLF1) MI 371 (Δ BBRF1), MI-80 (ΔBBLF4), MI-405 (ΔBBLF2/3), MI-317 (ΔBSLF1) and D-28 (ΔBMRF1), were gifts from Ya-Fang Chiu [46] . BM2710 bacteria were transformed with the above bacmids. BM2710 carrying EBV bacmids (Δ BcLF-1& Δ BBRF-1) were grown overnight for 16hrs at 32°C. HEK 293 cells in a 6-well dish at 70% confluency were infected with 500uL of the overnight grown culture for 2-3hrs at 37°C. The medium was aspirated and replaced with fresh medium. Gentamycin at 50 µg/ml was added. Two days later, the cells were split into 15cm dishes and two days later, 300ug/ml of hygromycin was added. Three weeks later, six colonies for each mutant were picked and expanded.

Induction of lytic cycle of HEK 293 cells carrying EBV bacmids

HEK 293 cells carrying EBV bacmids on 10cm dishes at 25% confluency were transfected with plasmids encoding immediate early genes BZLF1 and BRLF1 and a

late gene, p18, fused to GFP expressed from its native promoter [9] at a concentration of 1ug of total DNA/ 10^6 cells (2ug total DNA). Lipofectamine 2000 was used for the transfections at a ratio of 2uL of Lipofectamine/ ug of DNA.

3D reconstruction of live-cell images

Amira from Thermo Fisher Scientific and Imaris from Bitplane were used for reconstruction. The signals from various channels were manually thresholded and the signal intensities and volumes enclosed within the region thresholded were calculated. As a control, beads (from Abberior Instruments) ranging from 1um to 6um were used for reconstruction and the inaccuracies ranged from 100% to 2%, respectively.

Fluorescence In Situ Hybridisation (FISH)

FISH analysis was performed as described [47] . In brief, cells were treated with 0.075 M KCl for 20 min at 37°C, fixed in methanol:acetic acid at a 3:1 ratio for 30 min at room temperature, and spread on cold slides. Slides were dried and prehybridized in a buffer with 4× SSC and 0.5% (vol/vol) Nonidet P-40 (Sigma-Aldrich) for 30 min at 37°C, dehydrated in a cold ethanol series (70%, 80%, and 90%) for 2 min each, air-dried at 50°C, denatured in a buffer with 70% formamide and 2× SSC, pH 5.3, for 2 min at 72°C followed by dehydration with a cold ethanol series, and air-dried. A plasmid encoding LacO (2348) and one encoding LacI-tdtomato (4001.6) were labeled with digoxigenin-11-2′-deoxy-uridine-5′-triphosphate (Roche), and a plasmid encoding the HindIII C fragment of EBV [48] was labeled with biotin-16-dUTP (Roche) by nick translation as hybridization probes for detection of 4012 and P3HR1 in cells, respectively. 20 µL of the

labeled probe was precipitated along with 6 µg salmon sperm DNA and 4 µg human Cot-1 DNA (Invitrogen) and resuspended in 15uL of CEP hybridization buffer (55% formamide, 1× SSC, pH 7.0, and 10% dextran sulfate) followed by denaturation at 70°C for 10 min. 3-4uL of the probe was hybridized with each sample at 37°C overnight in a moist chamber. The slides were washed twice in 2× SSC containing 50% formamide for 30 min at 50°C and twice in 2× SSC for 30 min at 50°C. The hybridized probe was detected by incubation with 10 µl of a detection solution containing a mouse monoclonal anti-digoxin–FITC conjugate (Sigma-Aldrich) and a streptavidin-Cy3 conjugate (Sigma-Aldrich) for 20 min at 37°C. The slides were washed twice in 4× SSC containing 0.05% Triton X-100 for 5 min at room temperature and mounted in Vectashield antifading media with DAPI (Vector Laboratories) for staining chromosomes. FISH slides were imaged on a Leica Confocal STED microscope.

CHAPTER 3.

DETERMINANTS OF EPSTEIN BARR VIRAL DNA AMPLIFICATION DURING ITS LYTIC PHASE

Much of this chapter has been adopted from the paper by Nagaraju T, Sugden A & Sugden B (2019) PNAS. The computational simulations were carried out by Arthur Sugden and are included for better understanding of the chapter.

Introduction

Mammalian DNA synthesis is well-orchestrated to achieve consistent outcomes. Each DNA template is synthesized once and only once during each S phase [49]. Regions of DNA on the order of a megabase are synthesized with multiple internal sites of DNA initiation and completed independently of adjacent regions [50]. Chromosomes are synthesized in their entirety with the possible exception of a small number of their telomeric repeats [51]. DNA viruses, being obligate cellular parasites, have evolved to synthesize their genomes by capitalizing on different cellular components. Not only herpesviruses [7,52] but also adenoviruses [53] and parvoviruses [54,55] form discrete sites in the nuclei of infected cells in which they amplify their DNAs. These virus families have genomes spanning in length from 3 to 250 kbp and include both single- and double-stranded DNAs illustrating the diversity of cellular parasites that have evolved to revamp nuclear structure for their replication. It is not clear, though, what advantages this compartmentalization provides them. EBV DNA amplification has been examined to elucidate the role of replication compartments in the amplification of its DNA.

In latently infected cells, EBV DNA is synthesized similarly to cellular DNA with the significant exception that only ~85% of its genomes are duplicated each S-phase [47]. During the lytic phase, EBV, as with other herpesviruses, undergoes up to several hundred-fold amplification of its DNA [6,10,56] to provide the genomes to be housed in progeny viruses. The amplification is mediated by *cis* and *trans* elements - *cis* elements include the origins of DNA synthesis and the *trans* elements include replication machinery encoded by EBV and the cell. Its DNA amplification is carried out in replication compartments that are devoid of detectable histones including H2A, H3.1

and H3.3 [7]. While a single genome *per se* is insignificant compared to the size of the host genome, several hundred-fold amplifications generate a viral DNA mass approaching that of the host genome. Replication compartments which house the amplified viral DNA therefore significantly reorganize the landscape of the host nucleus. For example, the Herpes Simplex Virus-1(HSV-1) lytic phase correlates with an increase in the volume of the host nucleus by up to two-fold [52]. This reorganization of the nucleus facilitates transport of HSV-1 capsids [57].

While replication compartments can only be visualized via microscopy [7,57], examining DNA synthetic events often requires a population approach [6,17] . Another difficulty in understanding viral DNA amplification comes from its dependence on the cell cycle rendering it asynchronous in a population of cells [7,58]. To overcome these difficulties in understanding EBV DNA amplification, we analyzed two functionally distinct replicons in the same cells. Computational modelling was used to simulate features that fit their DNA amplification observed in bulk populations. The computational simulations made three striking predictions: 1) The lengths of the replicons could be compensated by the number of origins per template; 2) The initial number of viral DNA molecules determines their ultimate amplification; and 3) The cessation of amplification requires cessation of DNA synthesis *per se*. To test these predictions, single cell assays, including live-cell imaging, FISH and EdU-pulse labelling, in combination with population approaches were used with a cell line harboring two EBV DNA replicons, P3HR1 and 4012. These replicons are present in the same cells but differ in their lengths and numbers of origins. This testing confirmed the three predictions. P3HR1 and 4012 DNAs were synthesized to similar levels per unit of time, despite the

differences in their lengths and numbers of origins, consistent with the first prediction. The replication compartments were seeded by single genomes and each compartment amplified this single genome several hundredfold. The number of compartments that were seeded by P3HR1 and 4012 were proportional to the number of molecules of P3HR1 and 4012 that were present at the start of the lytic phase. During the 13-14 hours of DNA amplification in single cells, the replication compartments collectively eventually occupied 30% of the nucleus while the nuclei grew by 50%. Each replication compartment synthesized similar levels of DNA and therefore, the number of compartments directly determined the total DNA synthesized in each cell, consistent with the second prediction derived from the simulations. Early in this amplification process, DNA templates were a limiting factor for DNA synthesis. Late in the amplification process, unused DNA templates were in excess, coinciding with a drop in the levels of viral synthetic machinery in the replication compartments, consistent with the third prediction derived from the simulations. Our results establish that replication compartments represent clonal factories for DNA amplification that coordinate DNA synthesis during the lytic phase.

RESULTS

EBV DNA accumulation appears to be independent of the length of the template

iD98HR1-4012 cells harboring P3HR1, a 165 kb strain of EBV, and 4012, which is a 36 kb amplicon derived from EBV were used to study DNA amplification (Fig 2.1A). P3HR1 and 4012 are each present in multiple copies in iD98HR1-4012 cells - an average of ~ 25 copies of P3HR1 and ~ 5-10 copies of 4012 per cell, while the copy numbers vary between clones of these cells. 4012 contains 256 LacO repeats, encodes

the LacI-td tomato gene and has all the elements required in *cis* to support lytic DNA replication [7]. The needed *trans*-acting elements are encoded by P3HR1 and by the cell. Amplification of 4012 DNA gives increasingly intense, visible red fluorescent signals when observed by fluorescence microscopy. iD98HR1-4012 cells also express Z-ER which is a fusion protein consisting of the immediate early gene BZLF1 fused to the ligand-binding domain of the estrogen receptor [7]. Addition of tamoxifen to cells expressing Z-ER leads to translocation of the fused protein to the nucleus, where Z-ER initiates EBV's lytic phase. The levels of both P3HR1 and 4012 DNAs at different times after induction of the lytic phase were quantified by qPCR. These bulk measurements showed that the accumulation of both replicons was rapid from 10-20 hours post induction (hpi), then slowed, and eventually plateaued by 40 hpi (Fig 2.1B). Surprisingly, 4012 which is one-fourth the length of P3HR1 accumulated to a similar level as did P3HR1 (~50% of P3HR1) (Fig 2.1B). If the length of a replicon solely determined its rate of amplification, then 4012 would have outpaced P3HR1.

Encapsidation does not regulate DNA accumulation

Viral DNA accumulated most rapidly during the first 20 hpi followed by a slowdown in accumulation from 20 hpi to 40 hpi (Fig 2.1), and then plateaued. We tested if encapsidation could limit the late stages of viral DNA amplification by removing potential templates from DNA synthesis. This possibility could apply if EBV were to encapsidate its DNA as extensively as other herpesviruses do [59,60]. Furthermore, perhaps 4012 is preferentially encapsidated relative to P3HR1, explaining its surprisingly slow accumulation. Derivatives of EBV that could not form capsids or could not sequester DNA in capsids were assayed to learn if these defects abolished the

slowing accumulation of viral DNA during the lytic phase. HEK 293 cells maintaining EBV mutants which cannot express either the major capsid protein (BcLF-1) or the portal protein (BBRF-1) were generated and analyzed. The lytic phase was induced in the cells by transfection of vectors encoding the immediate early proteins BZLF1 and BRLF1. In addition, a plasmid encoding the minor capsid protein fused to GFP (p18-GFP) under the control of its native promoter was transfected to quantify the fraction of cells that supported the lytic phase. Neither of these induced cell populations released detectable, extracellular virions (Fig 2.2D), nor did they contain increased levels of EBV DNA when compared to induced cells carrying wild type EBV (Fig 2.2A). The inability of EBV to encapsidate its DNA, therefore is not sufficient to prevent the slowing accumulation of its DNA late in EBV's lytic phase. The number of intracellular and extracellular capsids measured from cells supporting wild-type EBV (Fig 2.2B, C) was similar to that found in other studies [61,62]. These measurements also showed that approximately 1% of each replicon was encapsidated (Fig 2.2B, C) ruling out the possibility that preferential encapsidation could explain the failure of 4012's synthesis to outpace that of P3HR1.

Modelling EBV's DNA amplification

We developed simulations to predict features of the DNA replication of 4012 and P3HR1 that led to their similar accumulation during the lytic phase (Fig 2.1B). The only additional data used in this modelling were measurements of the fraction of cells supporting the lytic cycle determined by the incorporation of EdU at each time point (Fig 2.3A; Table 2.1). Cells supporting EBV DNA amplification displayed distinctive EdU

signals which were confirmed by staining for viral replication proteins localized to the sites of amplification (Fig 2.3A). The simulations probed the following parameters: i) Replicons with short and long lengths, with one and two origins respectively were followed and their daughter molecules in individual cells per amplification cycle were tallied; ii) Initiation was allowed to be independent at each origin; and iii) Synthesis was not allowed to re-initiate at an origin until it was completed for that replicon. Three predictions of this model prompted further research. First, the model simulated the data best when the longer of the two replicons had two origins (Fig 2.3B). Under these conditions, the synthesis of the shorter replicon did not outpace that of the longer having two origins. When a longer replicon with only one origin was considered, the simulation predicted that the smaller replicon would outpace the longer replicon rapidly (Fig 2.3C). This prediction arises from the fact that a molecule that has two origins has a greater chance of being replicated due to higher chances of initiation compared to the molecule that has one origin. Therefore, despite the fourfold length difference in case of 4012 and P3HR1, the two molecules were predicted to take a similar time to complete an amplification of 500-1000-fold. Second, the overall levels of the two replicons synthesized were dependent on their initial numbers per cell prior to the onset of their amplification (Fig 2.3D, E). Third, the plateauing of the synthesis of each replicon late in the lytic cycle required the cessation of synthesis *per se*.

P3HR1 and 4012 are synthesized at similar levels; early and late lytic replication are regulated differently

The simulations predicted that DNA synthetic activity is similar for both P3HR1 and 4012 due to the number of origins and probability of the occupancy of these origins. If this prediction were correct, then similar numbers of molecules of P3HR1 and 4012 would be synthesized per unit of time despite the differences in length. To test this prediction, density shift experiments were used to follow the synthesis of P3HR1 and 4012 DNAs into daughter molecules. iD98HR1-4012 cells were pulsed with BrdU, a heavy thymidine analog, for increasing times beginning 8 hpi of EBV's lytic phase, the time when viral DNA accumulation could first be detected in density shift experiments. The cells were harvested, their DNA purified, sheared, and separated by equilibrium density centrifugation in CsCl gradients. The DNA in each fraction was measured by qPCR, detecting DNAs encoding BALF5 of P3HR1, LacI-tdtomato of 4012, and rhodopsin for cellular DNA. Pairs of cell cultures were labeled for 60 and 120 or 90 and 180 minutes (Fig 2.4A, C, F, G, J, K) and the experiments were performed with two biological replicates. To correct for the viral DNA present only in cells supporting EBV DNA amplification, EdU was used to identify cells undergoing viral DNA amplification. The EdU-pulse labelling experiments done in parallel to density shift assays provided a correction factor for interpreting the density shift assays. The density profiles of the separated DNAs demonstrated that both the fractions of the P3HR1 and of the 4012 DNAs increased in the heavy/light (HL) and the heavy/heavy (HH) portions of the gradients over time as a result of DNA replication in the presence of BrdU and

decreased accordingly in the light/light (LL) portions (Fig 2.4A-D,L-M); Tables 2.2 and 2.3). The LL portions also contained viral DNA from the cells that had not entered the lytic phase or entered it during the pulse time and masked the actual levels of the LL DNA remaining in only those cells supporting viral DNA amplification (Fig 2.4A-D, L-M; Table 2.2 and 2.3).

The numbers of P3HR1 and 4012 DNA molecules in the LL, HL, and HH fractions per cell supporting the lytic phase were measured (Table 2.2 and 2.3). The numbers per cell were derived by normalizing them to the cellular DNA detected with the rhodopsin probe and the fraction of the cells supporting the lytic cycle was determined by EdU-pulse labeling. These measurements revealed two striking findings. First the number of HL molecules at all time points early during the lytic phase for both P3HR1 and 4012 exceeded that of the LL molecules by about 10-fold. Effectively, 90% or more of all DNAs available were being used as templates. These analyses show that while 4012 DNA is one-fourth the length of P3HR1 DNA, the number of 4012 molecules per cell synthesized by the end of the labeling period (HL plus HH) was similar (60% of P3HR1) to the P3HR1 DNA synthesized (Table 2.2 and 2.3). These results indicated that at early times in the lytic phase, the number of available templates and the number of origins on each DNA but not its length correlated with the rate of viral DNA amplification, consistent with the predictions of the simulations.

Parallel experiments were conducted between 30 and 36 hpi, when approximately 60% of the cells supported EBV's lytic phase (Table 2.1). Even after labeling for six hours, a time twice that of the longest labeling period used early in EBV's lytic phase, the majority of both the P3HR1 and 4012 DNAs remained in the

unreplicated LL fraction (Fig 2.4B, D, H, I, L, M). These results indicated that at late time points EBV DNA synthesis is no longer regulated by the availability of DNA templates. This finding explains the slowing of accumulation of EBV DNA over time (Fig 2.1B). Similar numbers of 4012 DNA molecules (about 50%) were synthesized during the labeling period between 30 and 36 hpi as were P3HR1 DNA molecules (Table 2.4 and 2.5), consistent again with the predictions of the simulations.

We also tested the first prediction of the simulations by measuring the levels of EBV DNA amplification for three full-length replicons which have one origin of DNA synthesis, 2089, a derivative of the B95-8 strain, or two origins of DNA synthesis, the EBV strains, Akata and P3HR1. Akata and P3HR1 DNAs were amplified on average 6-8fold more than 2089 (Fig 2.4E) independently confirming the prediction that the number of origins per replicon of a given length affects its total accumulation.

Single cell assays demonstrate the clonality and coordination of DNA amplification in replication compartments

Analyses by qPCR (Fig 2.1B, 2.4E), computational modelling, and density shift assays (Fig 2.4A-D, F-M) established that both the rate and extent of DNA synthesis were similar for P3HR1, Akata and 4012 DNAs despite the functional differences in these replicons while that of 2089 DNA was predictably slower. In addition to highlighting a role for the number of origins per template during DNA synthesis, the simulations also predicted that the number of molecules at the beginning of the lytic phase was critical in determining the total DNA eventually synthesized. We

hypothesized that the number of molecules at the beginning of the lytic phase is proportional to the number of replication compartments formed. Single cell assays were used therefore to address two questions relevant to this hypothesis: Are replication compartments seeded by individual DNA molecules and do replication compartments coordinate their synthesis? To address the first question, FISH was used to detect P3HR1 and 4012 DNAs individually. We found that during the lytic phase, P3HR1 and 4012 were in their own compartments with only 0.2% of them being colocalized (in 1 out of 33 cells having on average 20 compartments per cell, only 1 compartment displayed colocalization (Fig 2.5B). (Colocalization is indicated by yellow signals). This finding indicates that single molecules serve as precursors for replication compartments. The replication compartments in some cases were adjacent to each other as has been observed for HSV-1 [63,64]. It is in these adjacent sites that viral recombination likely occurs as has been found for HSV-1 [64]. In addition, the number of compartments formed by P3HR1 and 4012 per cell correlated with the number of viral DNA molecules per cell at the beginning of the lytic phase (Fig 2.5A, B) showing that the number of viral DNA molecules present at the onset of the lytic phase correlated with the number of compartments ultimately formed. Counting the number of compartments in Fig 2.5B was restricted to cells with 30 replication compartments or fewer (90% of all cells) to maintain accuracy (in cells with >30 compartments, it was difficult to distinguish individual compartments resulting from their proximity with one another).

To address whether the number of compartments determined the overall levels of DNA synthesis and consequently the levels of DNA amplification, the cells were pulsed with EdU for 30 min at 37C at 13-14 hpi and analyzed. Replication compartments

seeded by 4012 DNA were reconstructed and EdU incorporation in these compartments was measured. The analysis was restricted to cells with 7 or fewer replication compartments containing 4012 (~80% of all cells) to ensure they were sufficiently distinct to be counted accurately (these cells had multiple, additional replication compartments housing P3HR1). The average levels of 4012 DNA synthesized were directly proportional to the number of 4012 compartments present indicating that the number of compartments determined the total DNA accumulated during the lytic phase (Fig 2.5C). Each replication compartment also supported similar levels of DNA synthesis indicating that each compartment, in addition to housing a single genome, apparently had the resources required for comparable levels of DNA synthesis. This interpretation was further supported by single cell assays measuring levels of BMRF1, the viral protein mediating the processivity of DNA synthesis in replication compartments. The level of BMRF1 (probed using an antibody to detect BMRF1) within the replication compartments increased early in the lytic phase in proportion to the volumes of the replication compartments and thus, in proportion to the newly synthesized DNA they contained (Fig 2.5D). Late in the lytic phase, the levels of BMRF1 decreased relative to the volumes of the compartments (Fig 2.5D), coinciding with majority of the DNA no longer serving as a template for DNA synthesis (Fig 2.4B, D). The observation that the distribution of BMRF1 within the replication compartments correlated with the number of viral DNA templates at times when 90% or more of the templates were supporting DNA synthesis indicates that the compartments are hubs in which DNA amplification is coordinated.

Single cell assays reveal the evolution of EBV's replication compartments over time

Live-cell imaging was used to follow viral DNA amplification in individual replication compartments and their DNAs were summed over time to define the time course of amplification in cells. The amplification of 4012 in replication compartments (Fig 2.6A) could first be detected between five and twenty-two hours after addition of tamoxifen in different cells. This broad range in time likely reflects that while EBV begins its DNA amplification at the G1/S border [7], the cells were asynchronously distributed throughout the cell cycle when tamoxifen was added. The peak accumulation of 4012 DNA took approximately 13 to14 hours on average in each cell (Fig 2.6A). We also found that after reaching peak intensity, the 4012 signals gradually decreased by 20-50%. This decrease in signal was not observed in cells that were not supporting the lytic cycle, making it unlikely that the decrease resulted from photobleaching. The decrease in 4012 signals also did not result from a loss of amplified viral DNA, as evidenced by the intensities of DAPI-staining within the compartments which increased throughout the lytic cycle (Fig 2.6D, E). A likely explanation for the late, observed decrease in the intensity of the tomato red signals is that its RNA is degraded by BGLF5 which is known to shut off host gene expression. For example, BGLF5 has been shown to shut off both GFP expression and that of many other genes [41]. The time course of viral DNA accumulation in a population of cells entering the lytic cycle (Fig 2.1B) therefore reflects the summation of the sigmoidal accrual of each replicon in single cells, each initiating asynchronously over 22-24 hours and lasting 13-14 hours.

The live-cell imaging also showed that replication compartments formed by 4012 occupied ~7% of the nuclear volume (Fig 2.6B). To extend this finding to include all compartments, we used EdU pulse-labelling and 3D reconstruction of the marked replication compartments. Approximately 30-35% of the nucleus was eventually occupied by all of the replication compartments (Fig 2.6C) while the nuclei grew by 50% in volume over the course of EBV DNA amplification (Fig 2.6B, C). This volume was consistent with the replicons together having accumulated approximately one-third the mass of the cellular DNA (Fig 2.1B) while the ratio of the final volume occupied by 4012 to that occupied by P3HR1 reflected the individual levels of their DNA accumulation. Thus, single cell assays establish that the volume of a given replication compartment is proportional to the amount of viral DNA in it (Fig 2.6B, C). Put together, the above results show that DNA amplification in individual cells proceeds for 13-14hrs after which it ceases as does the growth in volume of replication compartments. This cessation of amplification is consistent with both the eventual decrease in the fraction of DNA templates used for DNA synthesis (Fig 2.4B, E) and in the levels of the viral replication protein BMRF1 in compartments (Fig 2.5D). These findings, therefore, confirm the third prediction made by the simulations, that is, the plateau observed in DNA amplification in bulk measurements (Fig 2.1B) reflects the cessation of DNA synthesis *per se*. These analyses together reveal that replication compartments are hubs in which DNA amplification occurs clonally and coordinately.

Figure 2.1

A

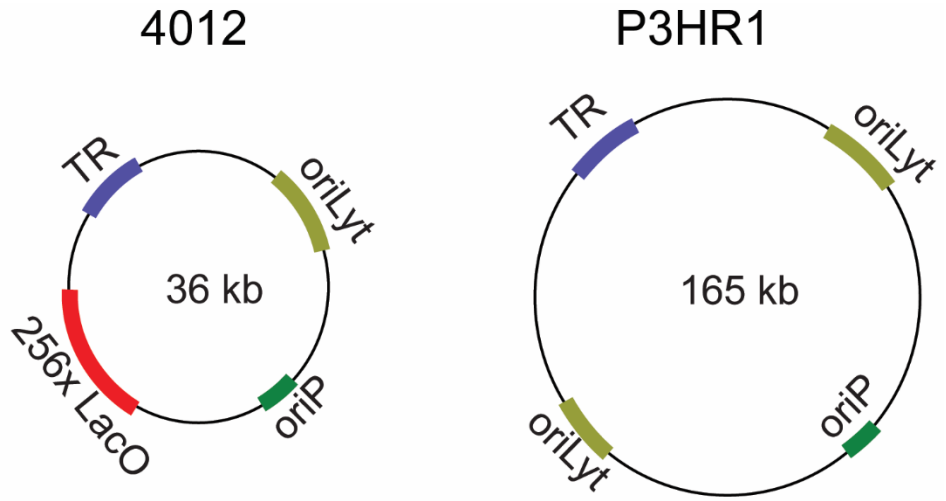
4012
TR
oriLyt
36 kb
256x LacO
oriP
P3HR1
TR
oriLyt
165 kb
oriLyt
oriP

B

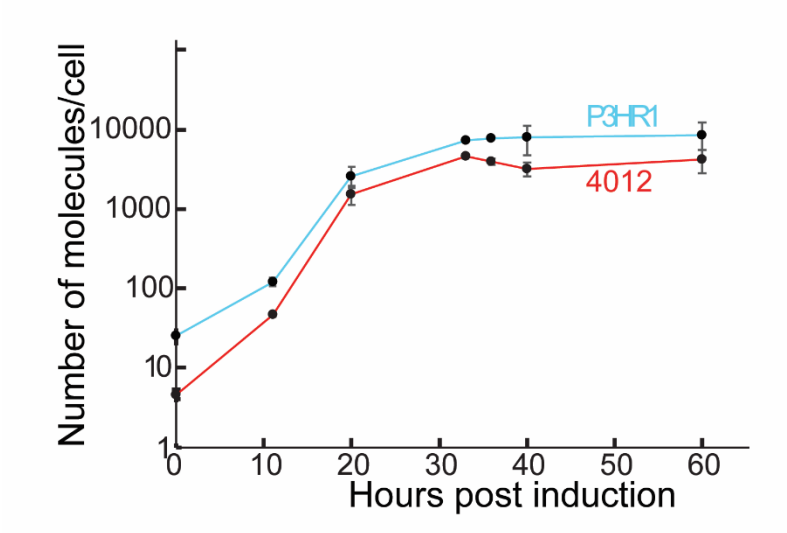
Number of molecules/cell
10000
1000
100
10
1
0
10
20
30
40
50
60
Hours post induction
P3HR1
4012

Fig 2.1. Measuring the synthesis of two replicons during EBV's lytic phase – **A**) The two replicons in iD98HR1-4012 cells are depicted. P3HR1 is a strain of EBV derived from the P3HR1 cell line and is 165kb in length. 4012, a derivative of EBV, is 36kb. The cis-acting elements essential for these studies are depicted and include oriP (latent origin of replication), oriLyt (the lytic origin of DNA synthesis), TR (the terminal repeats required for encapsidation of synthesized DNA) and LacO (the site to which the Lac Repressor binds). **B**) iD98HR1-4012 cells were induced to support the lytic phase by treatment with tamoxifen. The immediate early gene BZLF1 fused to the estrogen receptor is expressed constitutively in these cells. DNA was isolated from these cells at the indicated times and assayed for the amount of viral DNA and cellular DNA using qPCR (For time points 0, 20, 40, 60 hours post induction (hpi), n (biological replicates) = 4, for 11, 33, 36 hpi, n=2). The error bars indicate the standard deviation of the mean of the levels of EBV DNA / cell (with the assumption that each cell contains two copies of the rhodopsin gene).

Figure 2.2

A

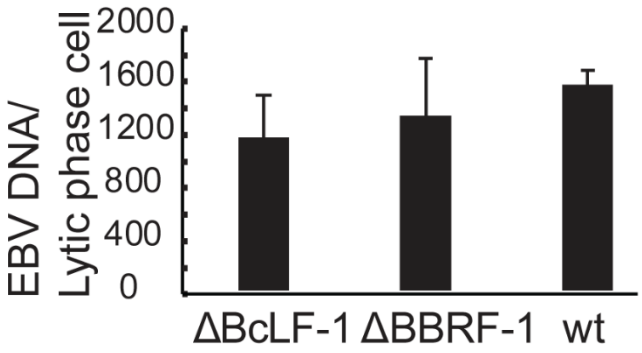

B

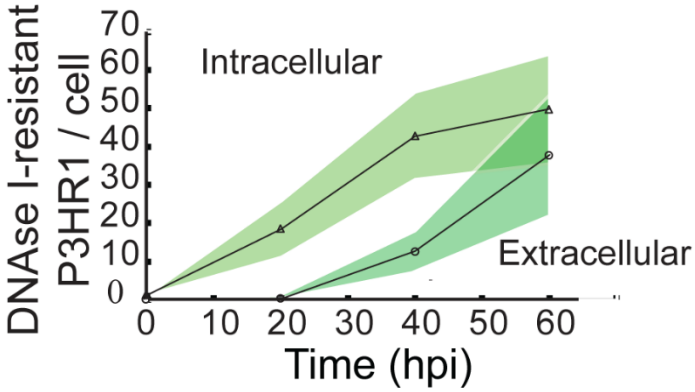

C

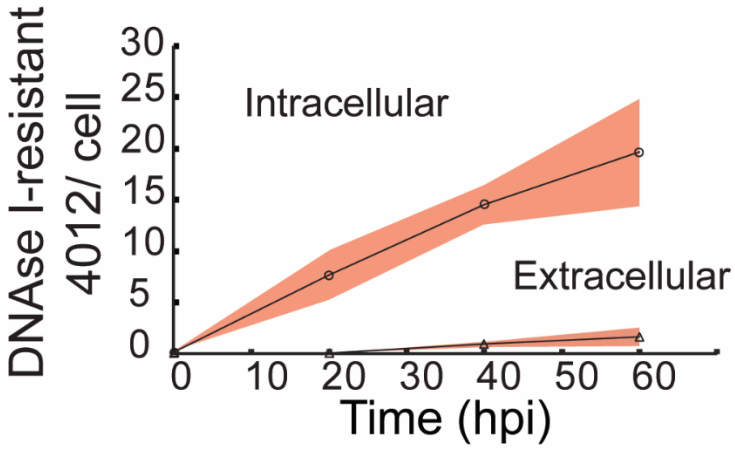

Fig 2.2 DNA encapsidation does not affect DNA accumulation- **A**) The levels of viral DNA synthesized in 293 cells harboring wt EBV or one of two EBV mutants were measured by qPCR at 48hpi. The mutants do not express either the portal protein, BBRF1, or the major capsid protein, BcLF1, and therefore cannot encapsidate viral

DNA. The lytic phase was induced by transfection of plasmids encoding the immediate early genes BRLF1 and BZLF1. In addition, a plasmid encoding the late gene product p18 fused to GFP was transfected to evaluate the fraction of cells supporting the lytic phase (n (biological replicates) =3, error bars indicate standard deviation). An unpaired student's t-test was carried out to determine p-values (p (BcLF1 vs wt) =0.1; p (BBRF1 vs wt = 0.4). **B&C**) The intracellular and extracellular encapsidated DNAs were assayed by measuring the levels of DNAseI-resistant P3HR1 and 4012 DNAs using qPCR at the indicated times from iD98HR1-4012 cells. n (biological replicates) =3 (the shaded areas indicate the standard deviation of the mean of the three biological replicates).

D

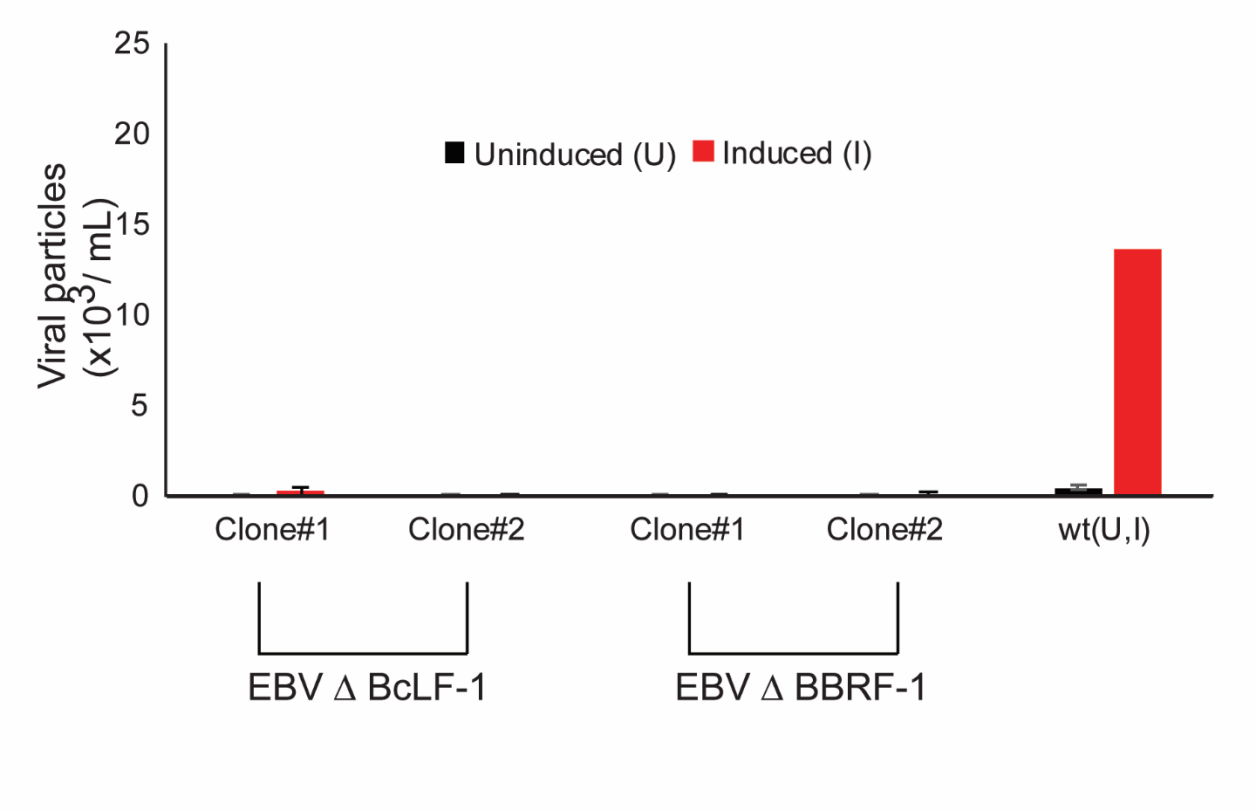

D) 293 cells carrying either the indicated mutant or wt derivatives of EBV were induced by transfection of plasmids encoding immediate early genes R and Z for the induction of lytic phase and a plasmid encoding a late gene product p18 fused to GFP to measure the fraction of cells supporting the lytic phase. The supernatant was collected at 96hpi and treated with DNAse I followed by addition of proteinase K and the DNA from the particles were purified and assayed using qPCR.

Figure 2.3

A

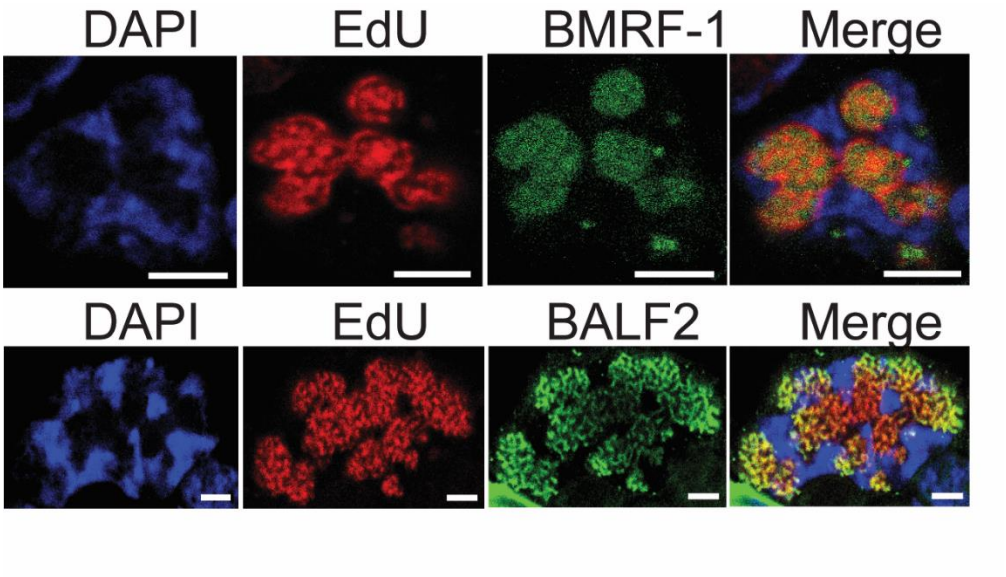
DAPI
EdU
BMRF-1
Merge
DAPI
EdU
BALF2
Merge

B

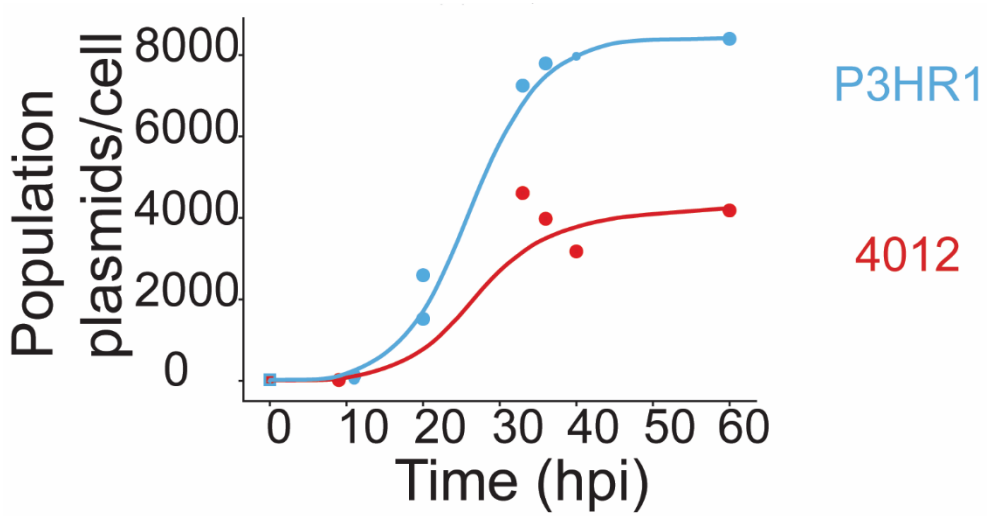
Population plasmids/cell
8000
6000
4000
2000
0
0
10
20
30
40
50
60
Time (hpi)
P3HR1
4012

Fig 2.3. Computational simulations predict the properties of DNA synthesis during the lytic phase – A) The fraction of iD98HR1-4012 cells supporting the lytic phase was measured using EdU incorporation. To establish that the detected, compartmentalized, EdU incorporation identified cells supporting the lytic phase, cells were also assayed for the early gene products BMRF1 (EBV DNA clamp protein), and BALF2 (single-stranded DNA binding protein) via immunofluorescence. They were detected only in cells exhibiting replication compartments as shown in A (scale bar-2µm). **B)** Shown is the best fit (in solid lines) of the optimal simulation of the measurements of Fig 2.1B (in data points) corrected for the fraction of cells supporting the lytic phase (Table 2.1).

C

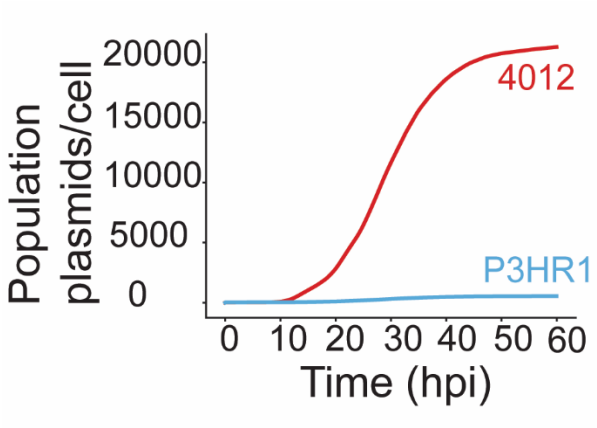
Population plasmids/cell
20000
15000
10000
5000
0
4012
P3HR1
0 10 20 30 40 50 60
Time (hpi)

D

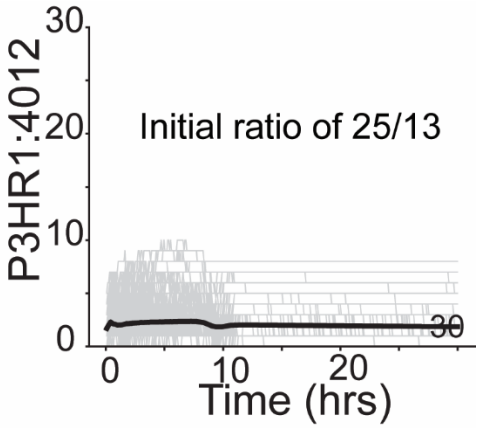
P3HR1:4012
30
20
10
0
Initial ratio of 25/13
30
0 10 20
Time (hrs)

E

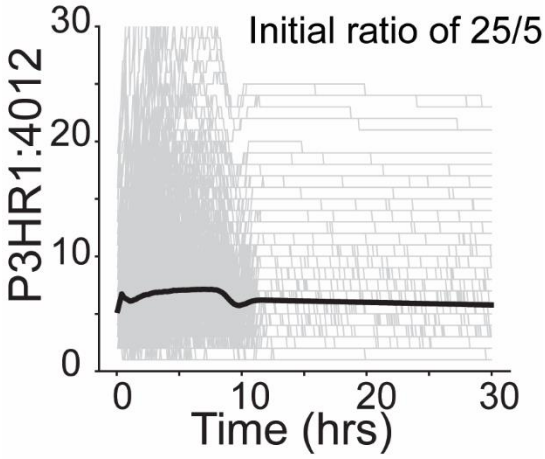
P3HR1:4012
30
20
10
0
Initial ratio of 25/5
0 10 20 30
Time (hrs)

C) The simulation predicts that were the P3HR1replicon to have only one origin, the 4012 replicon would amplify faster. **D&E)** Shown are the predictions of the simulation in which the initial ratios of P3HR1 and 4012 were varied in cells and found to determine the ultimate levels of their synthesis in each population. In grey, are shown the results of simulation of individual cells, with the solid lines reflecting the averages of all predicted cells.

Figure 2.4

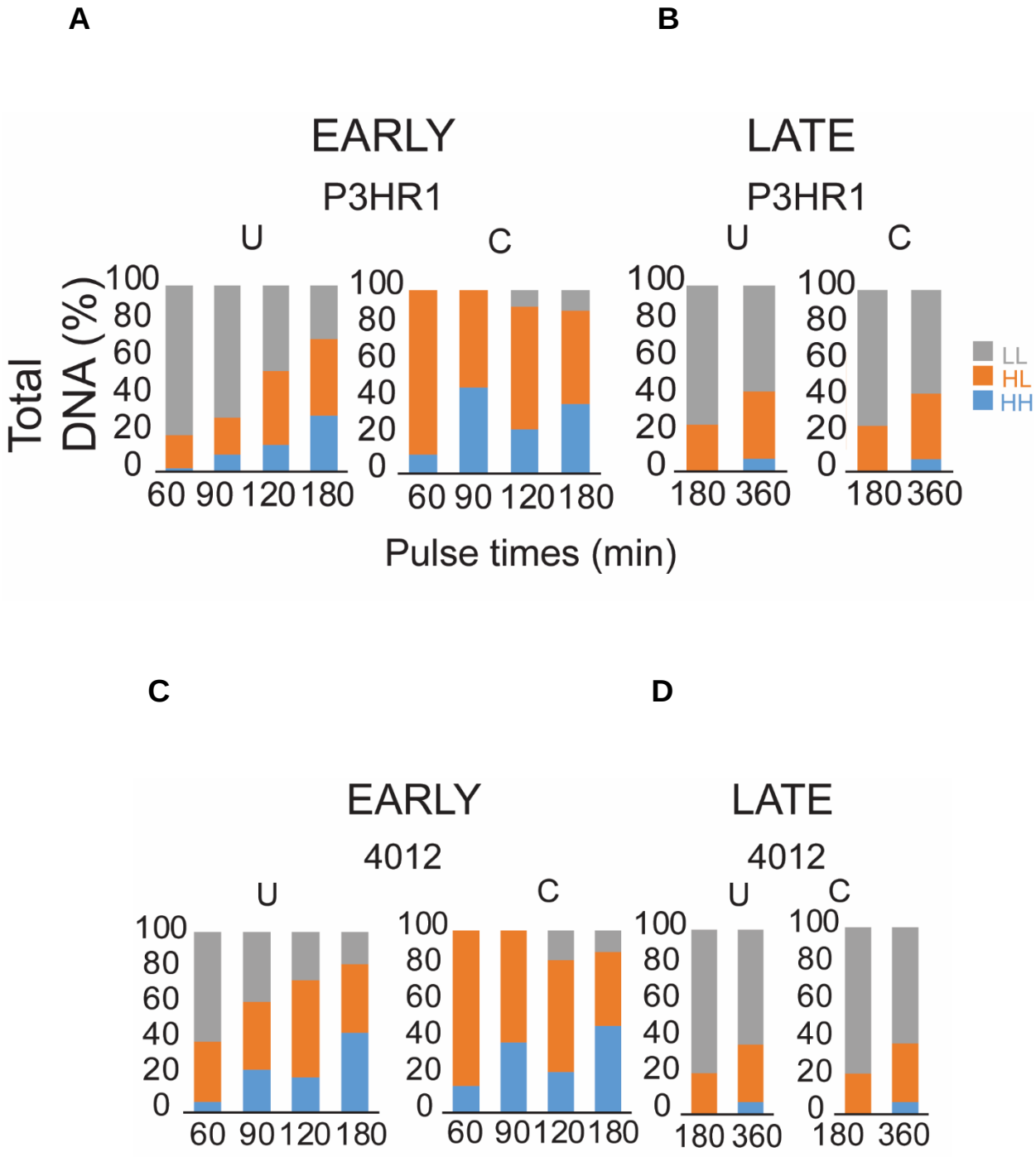

Fig 2.4. **Density shift assays reveal differences in DNA synthesis early and late during the lytic phase**- **A&B**) Bar graphs representing uncorrected (U) and corrected

(C) data from the density shift assays in which both P3HR1 and 4012 DNAs were measured with increasing pulse lengths at 8 hpi and 30hpi. The corrected values at 30-36hpi are close to the uncorrected values because most LL DNA is in the cells supporting the lytic phase. The density shift assay profiles are shown in F-M. The area under the curve for each peak is tabulated in Table 2.2-2.5. The density shift experiments were repeated two times and the mean of the area under the curves are represented in **A-D**. The fraction of BrdU labelled DNA was corrected for each sample by the fraction of cells supporting the lytic phase as determined in Table 2.1.

E

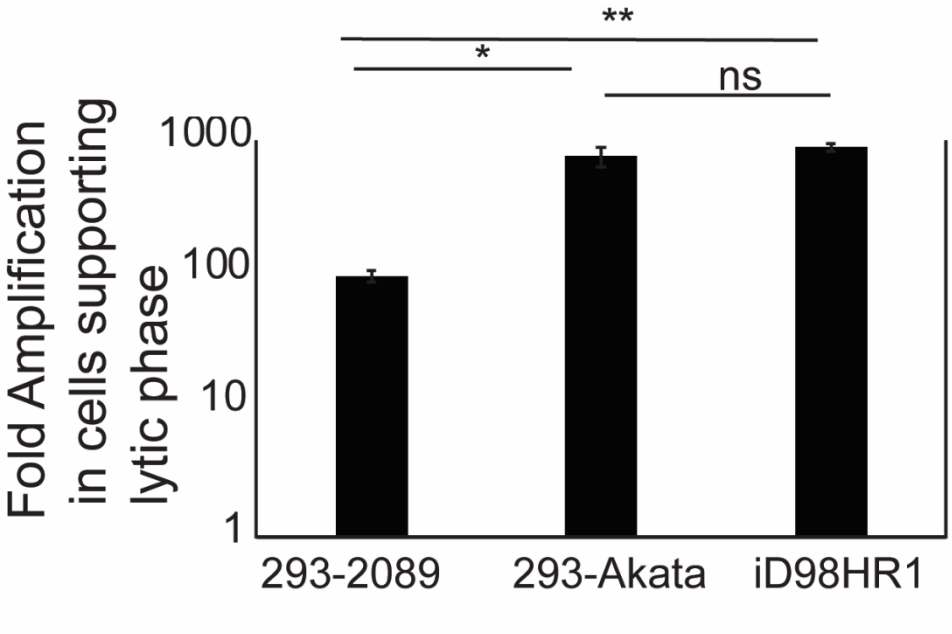

E) A bar graph representing quantitative measurements of total viral DNA per cell in cells supporting the lytic phase are measured using qPCR are shown. The different strains of EBV assayed are 2089 (a derivative of B95-8 which has one origin) in 293 cells, Akata (two origins) in 293 cells and P3HR1 (two origins) in iD98HR1 cells. (t-test-ns-not significant-p=.56; * p= .017; **p=0.0002).

F

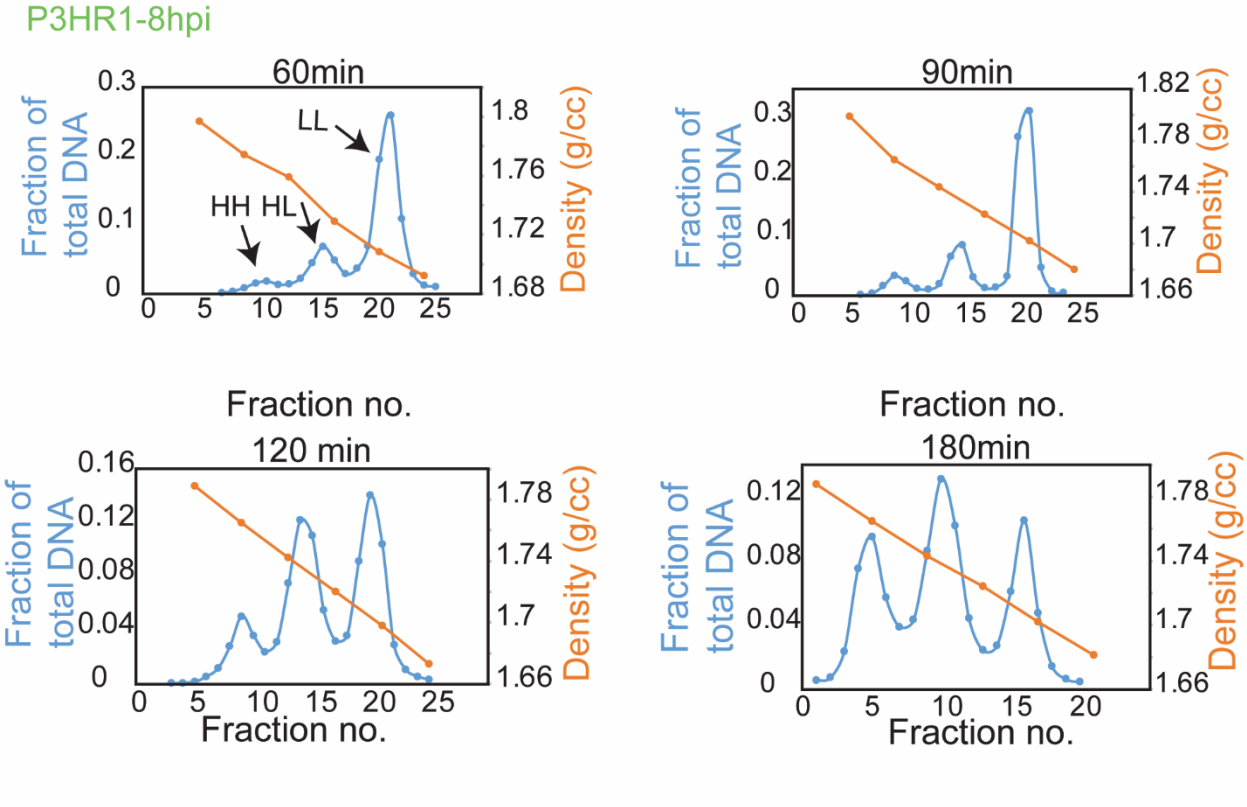

F) Density shift assay profiles for P3HR1 (replicate 1) respectively at the indicated pulse times early during the lytic phase (8 hpi). iD98HR1-4012 cells were induced with tamoxifen and labeled with BrdU at 8 hpi for indicated times. After induction, the DNA was isolated, sheared, separated in CsCl gradients and assayed using qPCR for viral DNA and cellular DNA as detailed in the Materials and Methods.

G

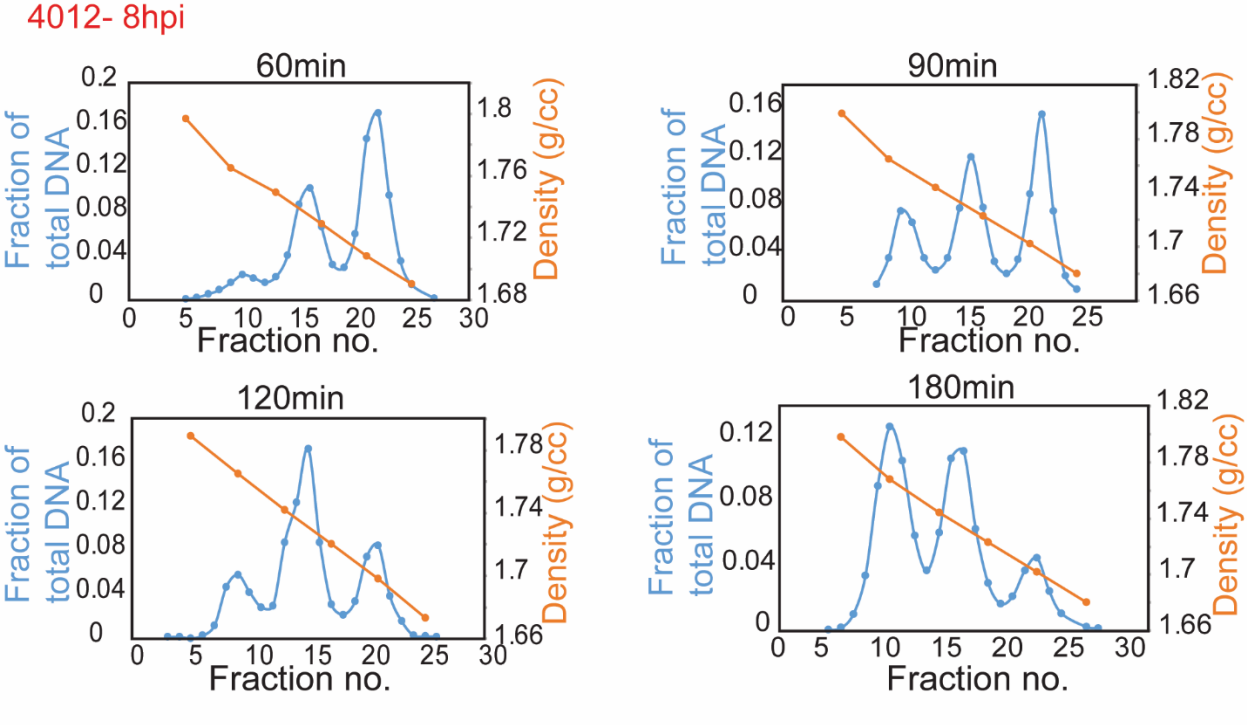

G) Density shift assay profiles for 4012 (replicate 1) respectively at the indicated pulse times early during the lytic phase (8 hpi). iD98HR1-4012 cells were induced with tamoxifen and labeled with BrdU at 8 hpi for indicated times. After induction the DNA was isolated, sheared, separated in CsCl gradients and assayed using qPCR for viral DNA and cellular DNA as detailed in the Materials and Methods.

H

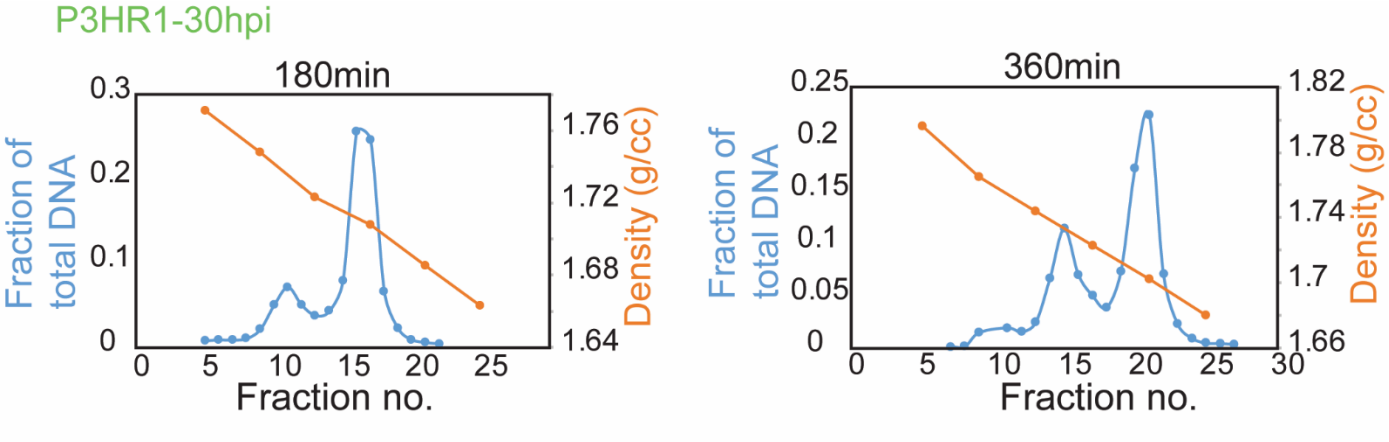

I

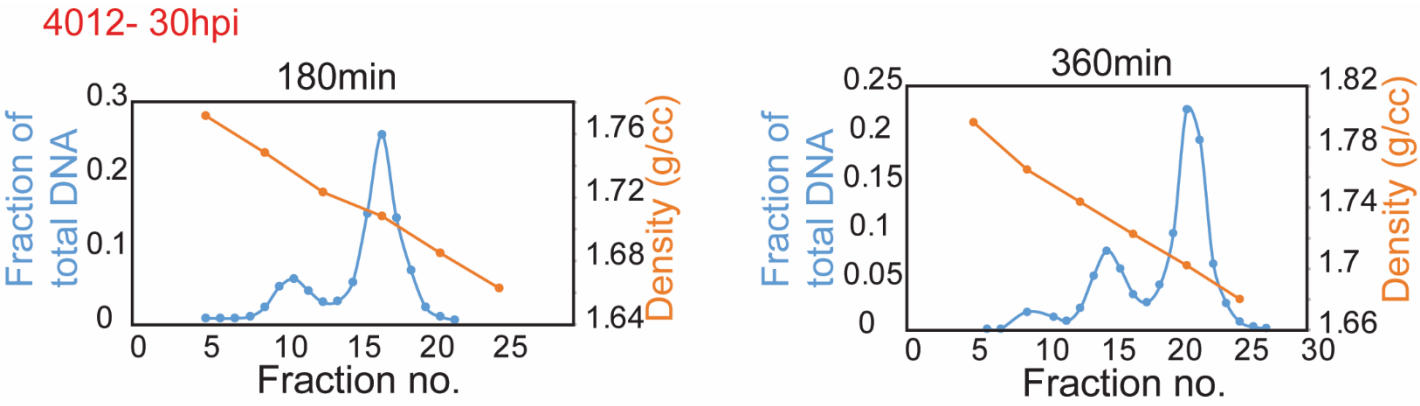

H&I) Density shift assay profiles for P3HR1 and 4012 (replicate 1) respectively at the indicated pulse times late during the lytic phase (30 hpi). The cells were processed as they were processed in A&B.

J

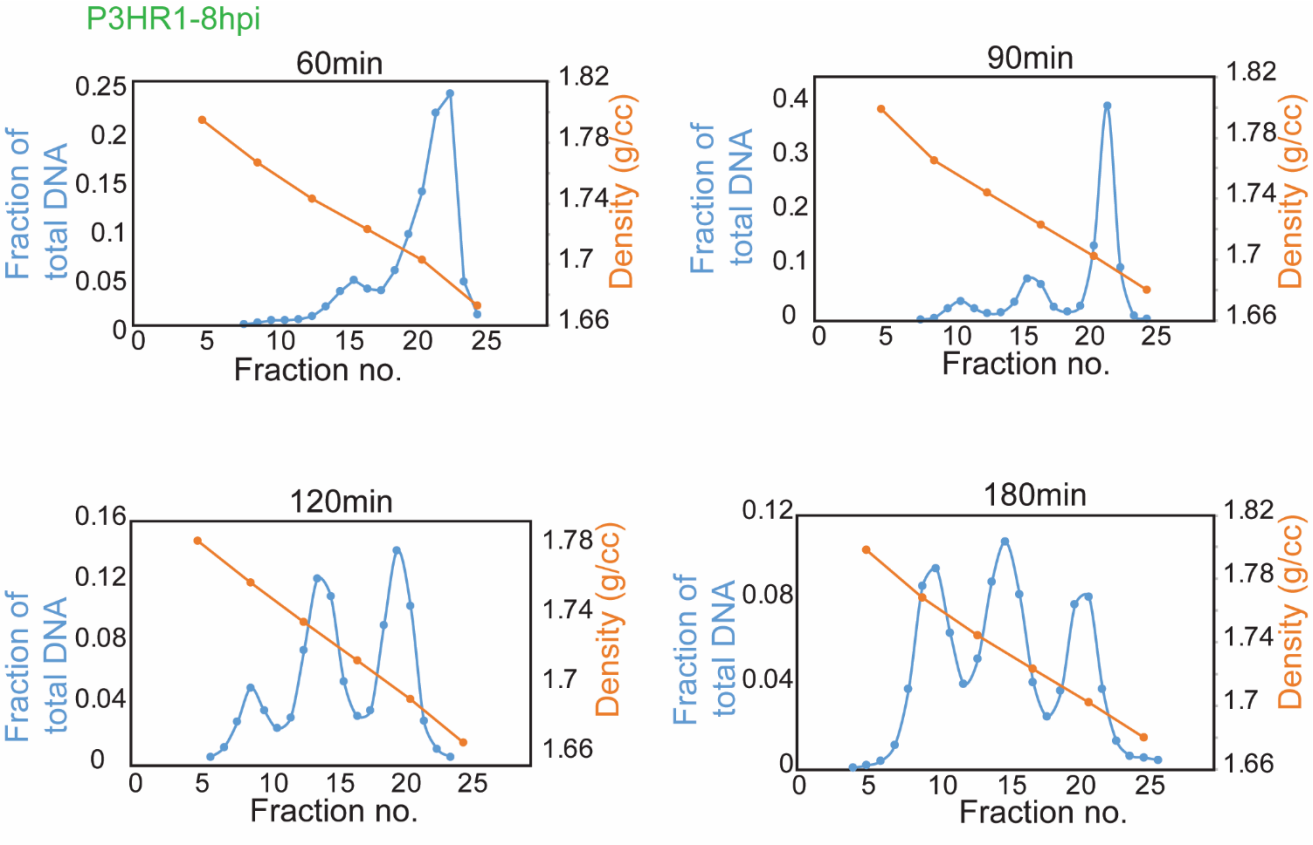

J) Density shift assay profiles for P3HR1 (replicate 2) respectively at the indicated pulse times early during the lytic phase (8 hpi). iD98HR1-4012 cells were induced with tamoxifen and labeled with BrdU at 8 hpi for indicated times. After induction, the DNA was isolated, sheared, separated in CsCl gradients and assayed using qPCR for viral DNA and cellular DNA as detailed in the Materials and Methods.

K

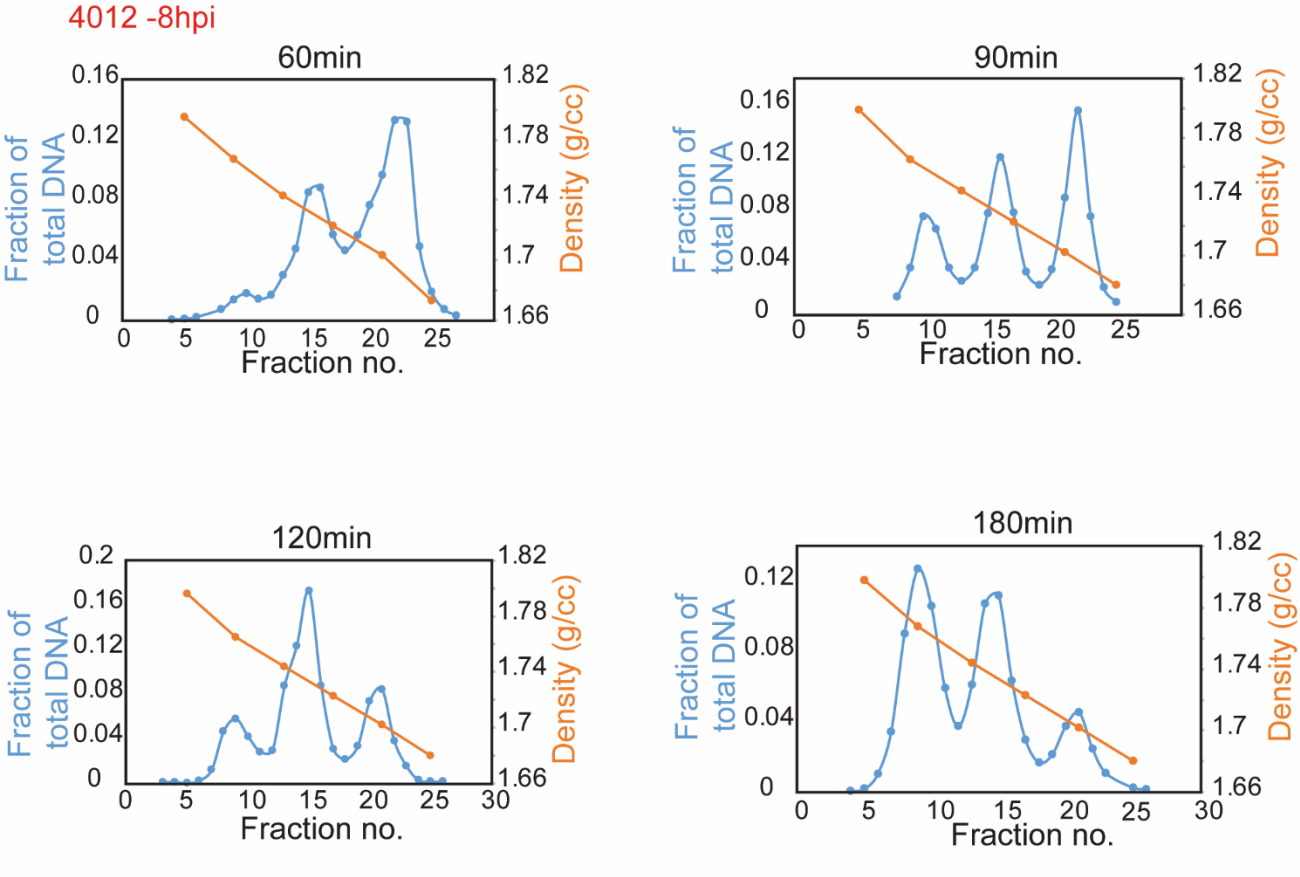

K) Density shift assay profiles for 4012 (replicate 2) respectively at the indicated pulse times early during the lytic phase (8 hpi). iD98HR1-4012 cells were induced with tamoxifen and labeled with BrdU at 8 hpi for indicated times. After induction the DNA was isolated, sheared, separated in CsCl gradients and assayed using qPCR for viral DNA and cellular DNA as detailed in the Materials and Methods.

L

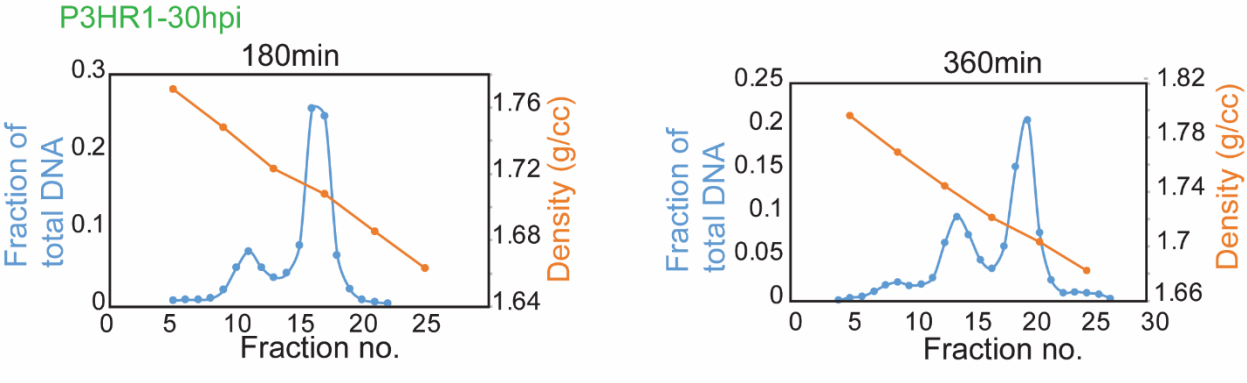

M

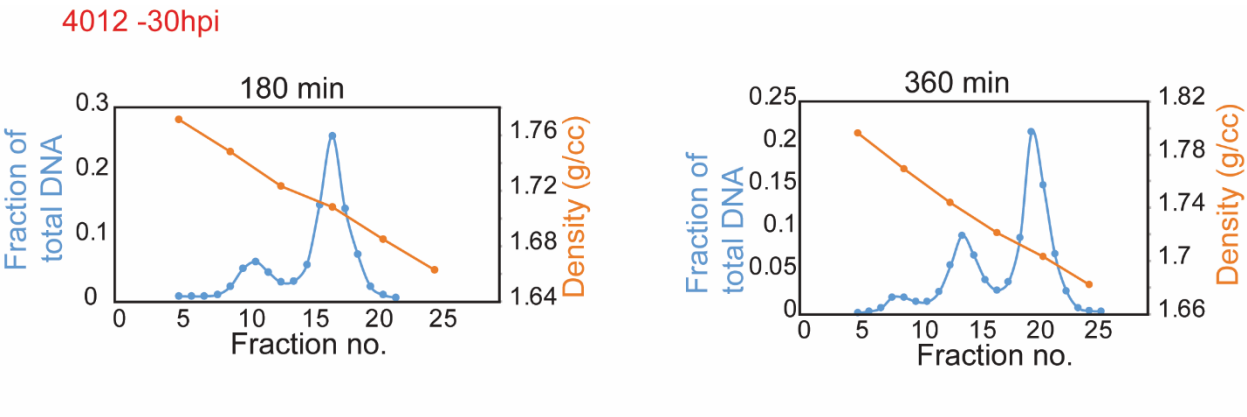

L & M) Density shift assay profiles for P3HR1 and 4012 (replicate 2) respectively at the indicated pulse times late during the lytic phase (30 hpi). The cells were processed as they were processed in A&B.

Figure 2.5

A

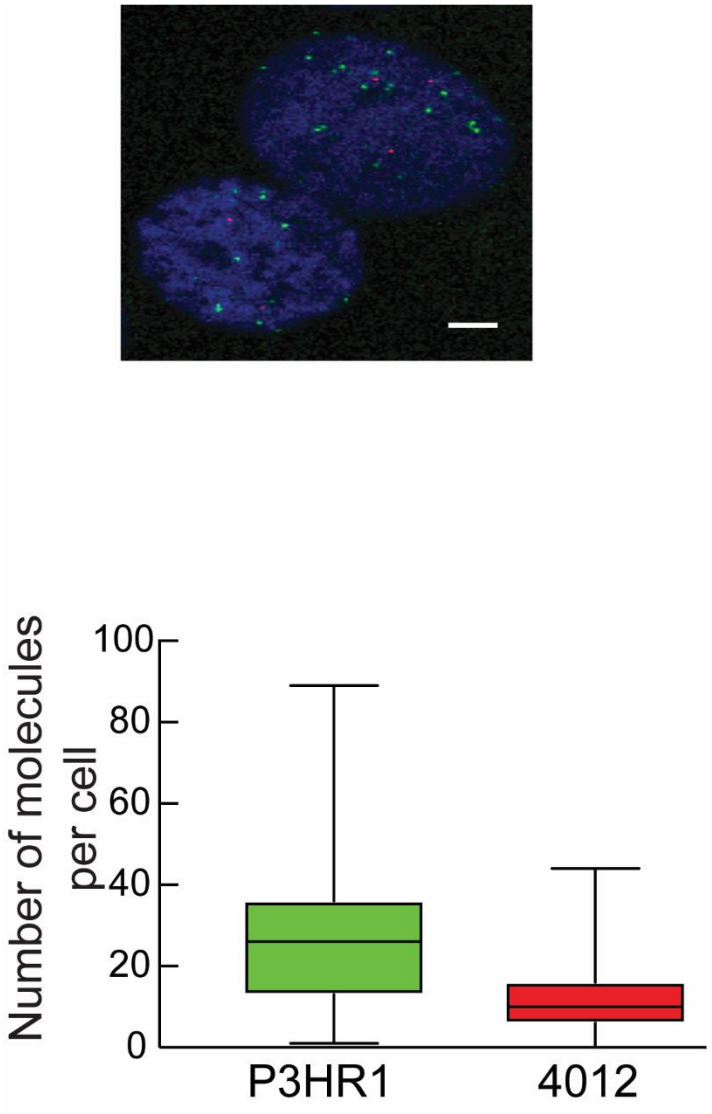

Fig 2.5. Single cell assays show that the number of replication compartments determine the levels of DNA amplification – A) Fluorescence In Situ Hybridisation (FISH) identifies P3HR1 (green) and 4012 (red) DNAs prior to the onset of the lytic phase

B

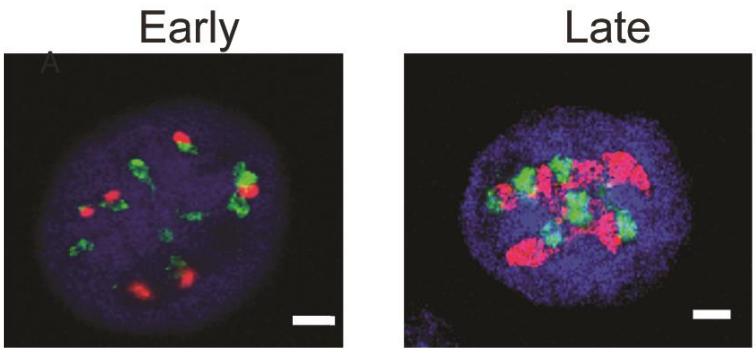

-

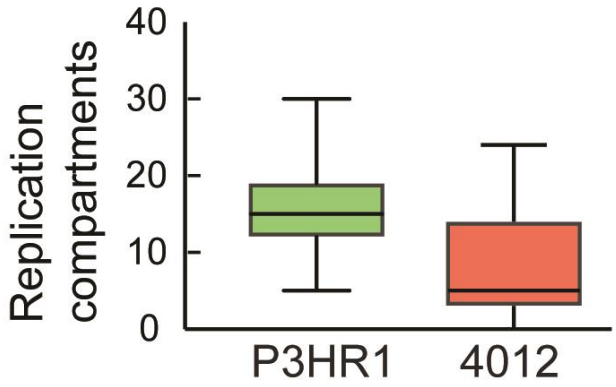

B) Fluorescence In Situ Hybridisation (FISH) identifies P3HR1 (green) and 4012 (red) DNAs during the lytic phase

C

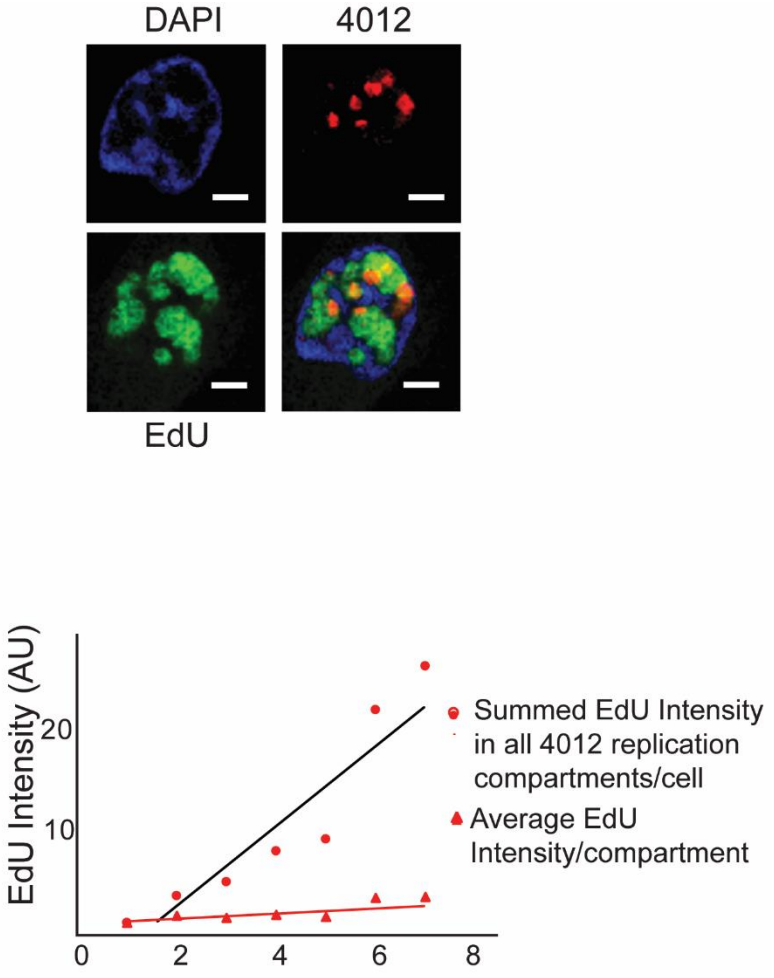

C) Quantitative analysis of 4012 DNA synthesis using EdU pulse-labelling and 3D reconstruction (n=51 cells). On the left is a representative image of a cell containing 4012 compartments in red and undergoing lytic DNA amplification as measured with EdU in green. The chromatin is represented by DAPI in blue. The black line (R^2=.88) indicates the average EdU intensity per cell having the indicated number of 4012

compartments on the x-axis. The red line (R^2= 0.75) indicates the average EdU intensity per replication compartment in any cell with the indicated number of 4012 compartments on the x-axis. Only cells with upto 7 compartments were counted to ensure the accuracy of counting. (Scale bar = 2μm).

D

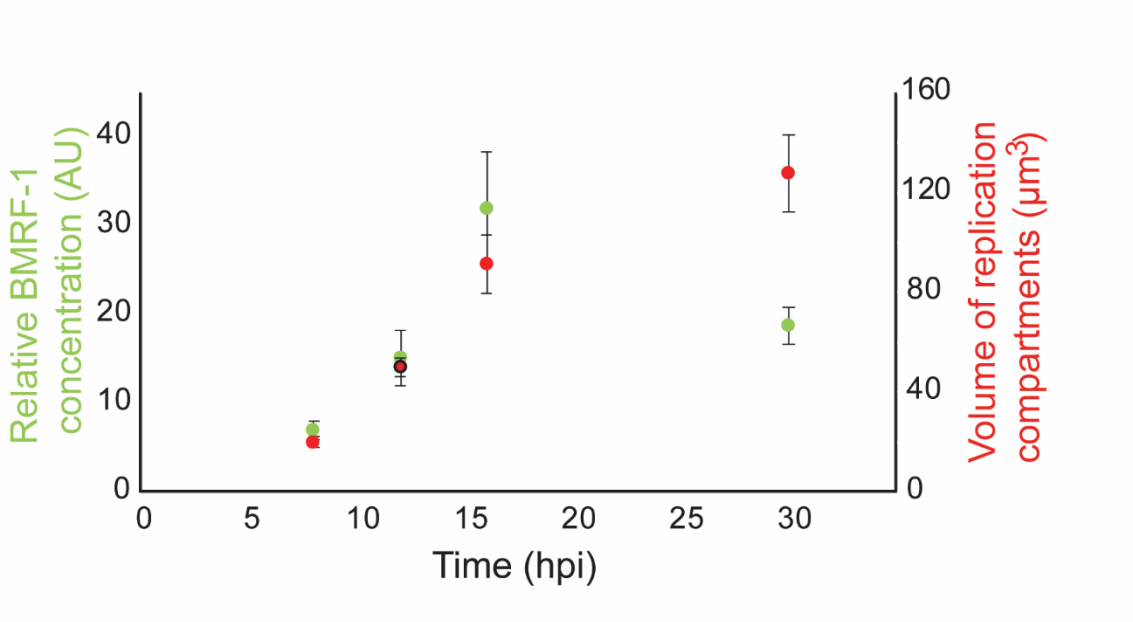

D) iD98HR1-4012 cells were induced with 200nM tamoxifen, fixed at the indicated times and probed with anti-BMRF1 antibody. The volumes of the 4012 compartments and the intensities of anti-BMRF1 staining in green were calculated by reconstruction of 4012 compartments (n=29-32 cells; error bars indicate standard error of mean)

Figure 2.6

A

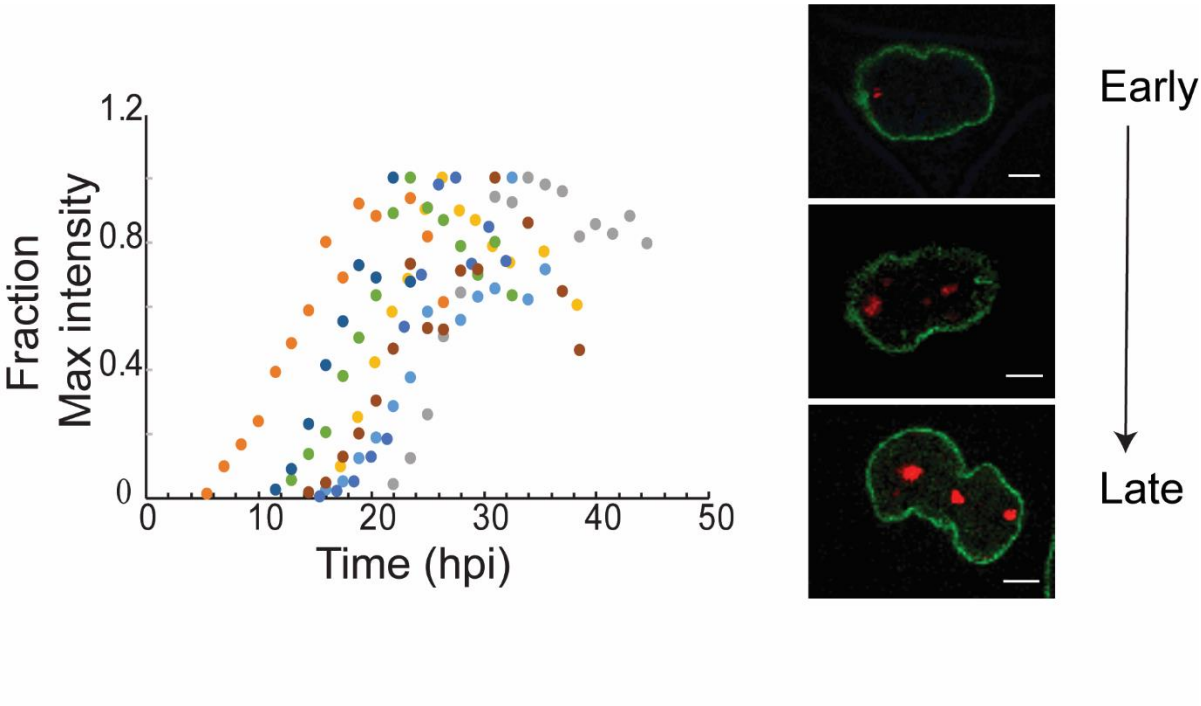

Fig 2.6. Single cell assays show spatial and temporal changes in the replication compartments during the lytic phase - A) iD98R1-4012 cells were induced to enter the lytic phase and followed from five to forty-five hpi. The replication compartments were then reconstructed and their total intensities was measured. Each colored dot represents the summed intensities of replication compartments in an individual cell at a given time. The fraction of maximum intensity (y) for the sum of all Replication-compartments for each cell was plotted as a function of time (x). The images on the right represent a single cell going through the lytic phase. Green indicates Lamin A/C-GFP which marks the nuclear membrane while red indicates LacI-td tomato which marks the replication compartments. Scale bar= 5µm.

B

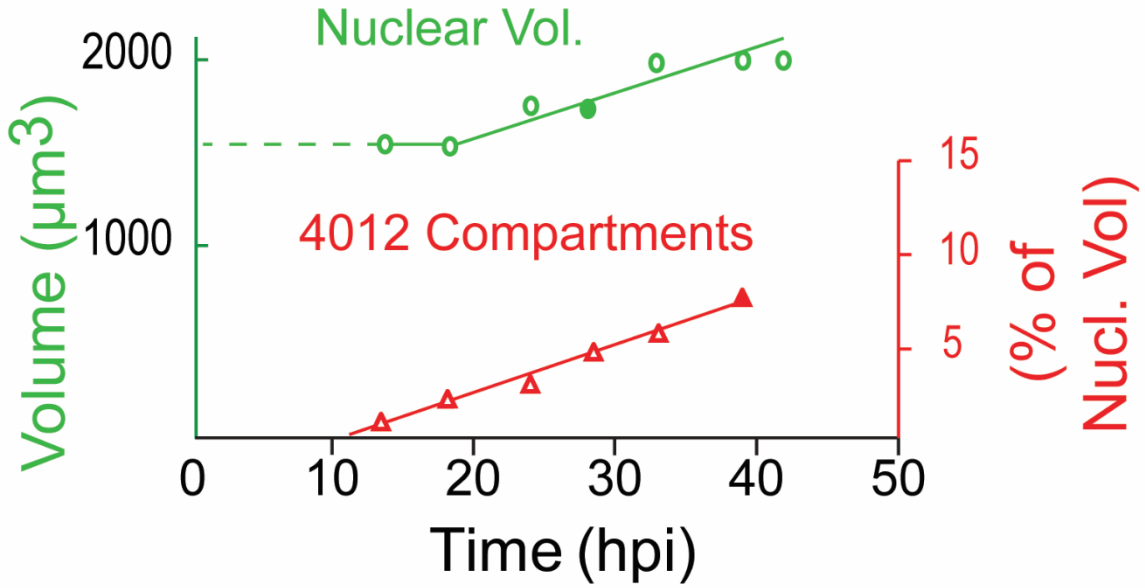

B) The volume of nuclei was measured by measuring the area within the Lamin A/C-GFP boundaries and summed over all the stacks (0.36µm/z-stack) for each time point, n=8 cells.

C

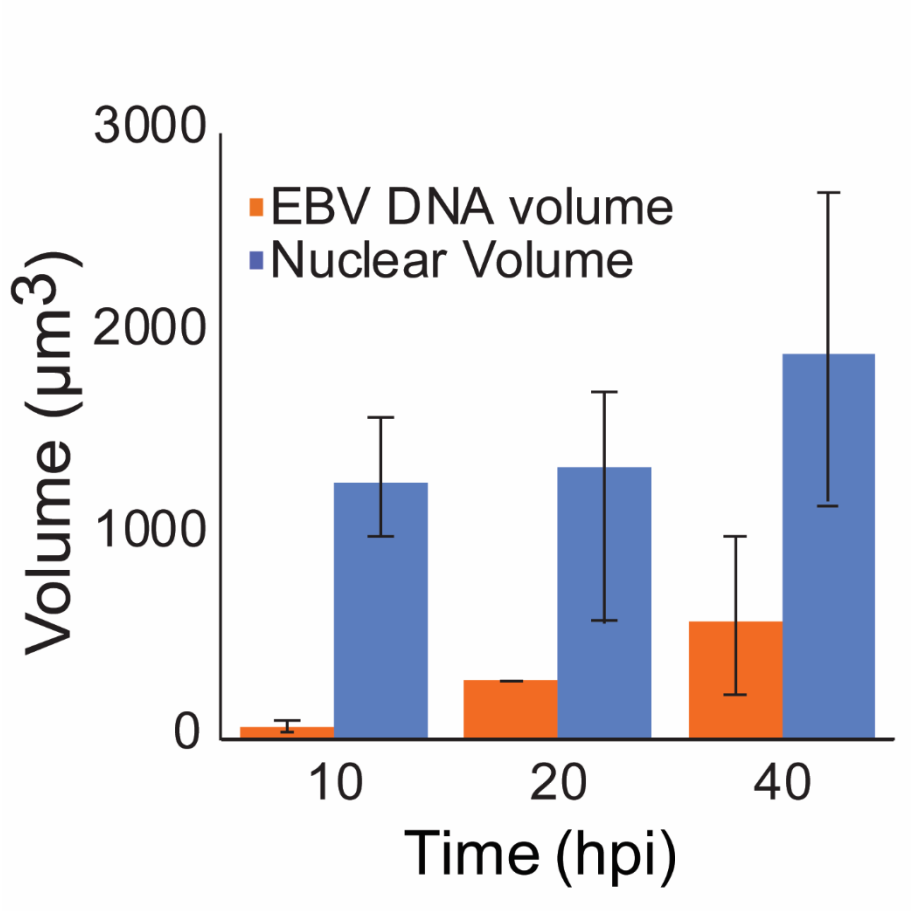

C) Cells were pulsed with EdU for 30 min at the indicated times after induction and the EdU and chromatin volume (DAPI) were reconstructed for 15-20 cells at the indicated times and the volumes were computed.

D

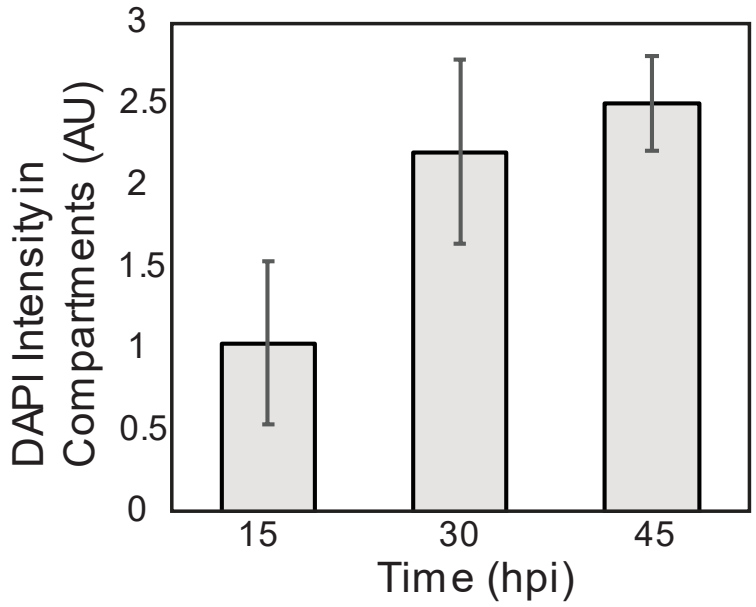

E

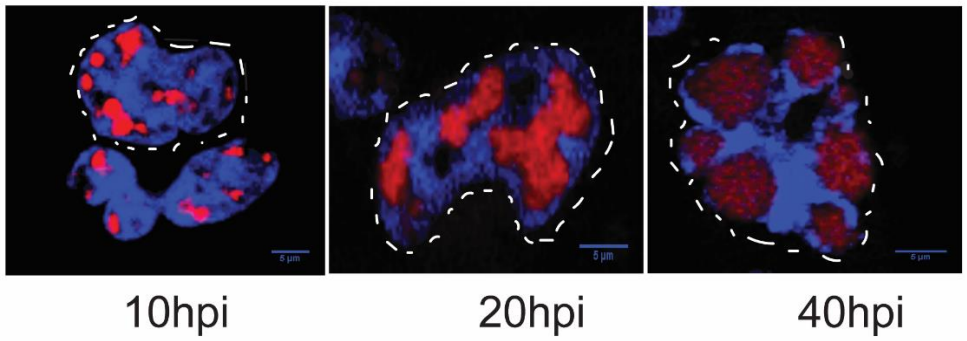

D) EdU was labelled by click chemistry (see Materials and Methods). The cells were then imaged. The total DAPI intensity inside the replication compartments (as indicated by EdU signals) was measured at indicated times (n=20-25 cells for each time point). Error bars indicate standard deviation. **E)** Illustration of cells pulsed with EdU at indicated times for 30 min.

Figure 2.7

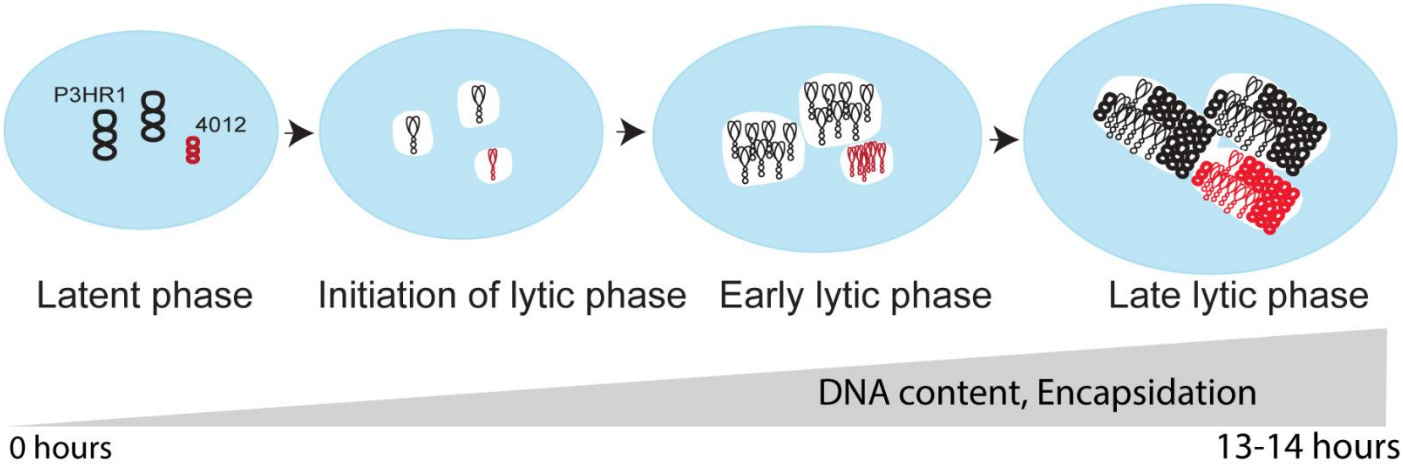

Fig 2.7. **A model for DNA amplification during the lytic phase-** During the latent phase, each molecule of EBV is replicated no more than once per cell cycle. The mature viral DNA (both P3HR1 in black and 4012 in red) are associated with chromosomal DNA represented in blue. On entering the lytic phase, each DNA molecule (shown as a replicative intermediate) has seeded a replication compartment (in white) which is devoid of cellular chromatin. During the early lytic phase, 90% of all viral DNAs are used as templates and compartments become juxtaposed but do not intermingle. Late in the lytic phase, the nuclear volume has increased by 50% and the compartments have occupied up to 30% of the nuclear volume. The compartments still haven't intermingled, only approximately 30% of the viral DNA serving as templates for DNA synthesis. The cellular chromatin is now restricted to the periphery of the nucleus. Late in the lytic phase, the ratio of each viral DNA (P3HR1:4012) remains similar to that

in the beginning in the lytic phase illustrating the coordination of DNA amplification by replication compartments. The amplified DNA is associated with and becomes encapsidated by viral particles late in the lytic phase.

Table 2.1

	BrdU Pulse time (min)	Fraction of cells supporting lytic phase
8hpi	60	0.03
	90	0.13
	120	0.07
	180	0.15
30hpi	180	0.6
	360	0.6

Table 2.1. Fraction of cells that support EBV's lytic phase- The fraction of cells supporting the lytic phase at the indicated time hours post induction (hpi) for cells pulsed in parallel with EdU were measured and used as correction factors for density shift assays. 60 and 120min pulses beginning at 8 hpi are a pair and 90- and 180-min pulses beginning at 8hpi are a pair of measurements each having two biological replicates. The correction factors are averages of their biological replicates. For each of these biological replicates, four technical replicates were used.

Table 2.2: P3HR1 (8hpi)

Pulse times (min)	Replicate	LL (molecules/Rho)	HL (molecules/Rho)	HH (molecules/Rho)
60	1	0	22	2
	2	0	48	12
90	1	0	12	10
	2	0	11	5
120	1	2	180	65
	2	3	238	70
180	1	5	156	116
	2	7	200	111

Table 2.3: 4012 (8hpi)

Pulse times (min)	Replicate	LL (molecules/Rho)	HL (molecules/Rho)	HH (molecules/Rho)
60	1	0	34	6
	2	0	25	5
90	1	0	15	9
	2	0	12	9
120	1	3	137	50
	2	2	158	55
180	1	3	72	84
	2	3	84	93

Table 2.4: P3HR1 (30hpi)

Pulse times (min)	Replicate	LL (molecules/Rho)	HL (molecules/Rho)	HH (molecules/Rho)
180	1	3638	1234	NA
	2	3561	1126	NA
360	1	3038	1915	381
	2	2932	1668	275

Table 2.5: 4012 (30hpi)

Pulse times (min)	Replicate	LL (molecules/Rho)	HL (molecules/Rho)	HH (molecules/Rho)
180	1	2076	590	NA
	2	2014	517	NA
360	1	1923	975	209
	2	1729	805	175

Table 2.2-2.5- Measurements of viral and cellular DNAs in density shift experiments: Cells were labelled with BrdU for increasing times at 8hpi (Table1-2) and 30hpi (Table 2.3- 2.4); DNAs were isolated from them, separated by CsCl equilibrium centrifugation and detected by qPCR as described in the materials and methods. Profiles of the assays of each gradient are shown in Fig S3 A and B. Each fraction in

each gradient was assayed for P3HR1 and 4012 DNA it contained and its density. Each set of DNAs labelled for a given was isolated from cells also assayed for the extent of their support of the lytic phase using EdU pulse labelling as described in the materials and methods. The tabulated numbers indicate the amount of each type of viral DNA normalized to cellular DNA (Rho) loaded onto the gradient and found in the peaks of light/light (LL), heavy light (HL) and heavy heavy (HH) densities after correction for the fraction of cells supporting the lytic phase in that sample.

CHAPTER 4.

DETERMINANTS OF CHROMATIN REORGANIZATION DURING EBV'S LYTIC PHASE

Introduction

During the lytic phase, herpesviruses, in addition to amplifying their viral genome, also reorganize the host chromatin. The viral DNA amplification and reorganization of chromatin happen concurrently in spatially non-overlapping regions. About the time the viral DNA has been amplified 500-1000 fold, the chromatin is marginalized to the periphery of the nucleus. This reorganization of chromatin (ROC) has also been observed in infections by other family of DNA viruses including adenoviruses, parvoviruses and baculoviruses[65]. The mechanisms underlying this phenotype have not yet been defined.

Some studies have found that signaling pathways[66] for DNA damage and for apoptosis[67] alter chromatin territories in the nucleus. Moreover, viral proteins expressed by EBV[68,69] and KSHV[70,71] are known to interact with these pathways. Several papers have shown that many DNA damage proteins localize to viral replication compartments and aid viral DNA amplification[71]. In addition, viral proteins have also been known to interact with several chromatin remodeling proteins that alter chromatin structure[72]. However, all these data are purely correlative and therefore provide no clear mechanism or determinant(s) for the reorganization of chromatin.

Recently, it was shown by Quincy Rosemarie, a graduate student in the lab, that continuous EBV DNA replication is not required for ROC (contrary to another study[40]), but instead only the initiation of DNA replication is needed. 293 cells harboring an EBV mutant lacking oriLyt did not support ROC on induction of the lytic phase (by

transfection of Z and R). However, cells harboring EBV supported ROC in the presence of ganciclovir, a potent inhibitor of viral DNA elongation . This finding suggests that an early event during the lytic phase, and not continuous DNA replication, likely triggers the reorganization of chromatin. I have developed a genetic approach to tease apart the viral factors required for this process.

Results

Development of cell lines harboring EBV mutants for early genes

From Quincy's studies we conclude that some aspects of initiation are likely triggers for ROC and therefore, we wanted to systematically test each of the viral genes that are involved in the initiation of DNA replication (Fig 1.1). Dr. Ya-Fang Chiu provided us with the following EBV mutants in which insertion of Tn10 transposons abrogates the expression of specific genes:

1) EBV ΔBBLF4 – BBLF4 is a helicase that is required for DNA synthesis
2) EBV ΔBMRF1 – BMRF1 is a processivity factor for the viral replication polymerase
3) EBV ΔBSLF1 – BSLF1 is a primase that facilitates viral DNA synthesis
4) EBV ΔBBLF2/3 – BBLF2/3 is a protein that tethers the viral replication complex to the origin of DNA replication, oriLyt

Once the bacmids were obtained in EPI 300 bacteria, individual colonies were screened for the integrity of the DNA sequence by restriction analysis using the restriction enzymes BamHI, PvuI and Xba1. BamHI cuts the viral DNA several times while XbaI and PvuI cut the viral DNA only a few times. Therefore, the two patterns

complement and likely give a complete picture of the digested DNA. Subsequently, these DNA were sequenced using high-throughput Illumina sequencing. The sequence accuracy was confirmed and BM2710 was transformed with sequence-verified bacmids. BM2710 is a strain of E.coli that expresses invasion genes of *Yerisinia tuberculosis* and listerolysin of *listeria monocytogenes* that permit the entry of the bacteria by a phagocytic uptake by a subset of adherent cells[73,74]. The BM2710 clones were analyzed the same way as the EPI 300 clones for the integrity and sequence accuracy of the bacmid DNAs. Bacteria carrying the appropriate bacmids were used to infect 293 cells. The protocols for the above experiments have been described in Chapter 2.

	Gene Mutated (Technical name)	Location on the genome (bp)	Type of mutation	Number of clones
1)	BBLF4 (MI-80)	101041	1.2 kb Kanamycin cassette insertion	3
2)	BMRF1 (D-28)	67656	2kb Apramycin cassette insertion	4
3)	BSLF1 (MI-317)	72918	1.2 kb Kanamycin cassette insertion	6
4)	BBLF2/3 (MI-405)	106720	1.2 kb Kanamycin cassette insertion	3

Table 4.1 EBV mutants verified and stably maintained in 293 cells: All the above mutants have been sequenced to confirm the integrity of the sequence

FUTURE DIRECTIONS:

We have generated three to six clones of these mutants in 293 cells and need to evaluate the fraction of cells in each clone that support the lytic phase. This evaluation can be made by transfecting R, Z and the deleted gene for each EBV mutant. These cells can then be pulsed with EdU at 48hrs and imaged to evaluate the fraction of cells that support the lytic phase (Refer to Chapter 2 and 3 for more details). Subsequently, two clones (for each mutant) that support the lytic phase efficiently will be analyzed for reorganization of chromatin by transfecting the cells with R, Z, and H2B-GFP +/- the deleted early gene. The levels of reorganization of chromatin in each case will be analyzed using ROC-QUANT, a program Quincy Rosemarie has developed to quantify the reorganization of chromatin.

To summarize, Quincy has found that continuous DNA replication is not required for ROC. In addition, she has also shown that oriLyt on the viral genome is required for the reorganization of chromatin. This suggests that initiating events of DNA synthesis are required for ROC. Once the cell lines I have generated are tested for their ability to support ROC, we will be able to elucidate the initial aspects of DNA synthesis (such as initiation or priming for DNA synthesis etc) that will be required for ROC.

CHAPTER 5.

FUTURE DIRECTIONS

Herpesviruses such as Herpes Simplex Virus-1 (HSV-1), human Cytomegalovirus (hCMV), Epstein-Barr Virus (EBV) and KSHV undergo massive DNA amplification of 500-1000 fold during their lytic phase[6,75]. DNA amplification is necessary for subsequent late gene transcription and packaging of the viral genome. To study DNA amplification and factors that quantitatively regulate it, EBV was used as a model. EBV provides a tractable model to study the transition of herpesviruses from their latent phase to their lytic phase. Some of the determinants that control the levels of EBV DNA amplification in cells during the viral lytic phase have been identified. We have shown that the number of EBV molecules present in a cell during latency and the number of origins each molecule harbors quantitatively regulate DNA amplification. Our work provides a paradigm for understanding DNA amplification of other herpesviruses including KSHV, HSV and hCMV, all of which are human pathogens and are known to cause multiple diseases.

In this section, I will discuss questions which if addressed, will build on our studies. These questions have not been addressed in the past largely due to technical difficulties. We can now address several of these questions using new techniques.

Several complex factors control viral DNA synthesis during the lytic phase of herpesviruses. Understanding these factors would shed light on developing therapeutics to prevent diseases caused by these herpesviruses. We have found that the amount of viral DNA amplified is directly proportional to the number of origins on a viral genome. It is known that the origin, oriLyt, is required at least for the first round of DNA replication. However, its role is not clear after the first round of DNA replication. One associated question is: what is the role of a defined origin (O) throughout the lytic phase? (oriLyt for

hCMV, EBV, and KSHV and oriL and oriS for HSV-1). What is the role of O in DNA synthesis after the first round(s) of DNA replication? Cell lines harboring mutant virus that harbor O flanked by Cre-lox sites can be synchronized within the cell cycle by a temperature variation method [76]. These cell lines will also require the expression of a fusion protein Cre-ER. The addition of tamoxifen induces translocation of Cre into the nucleus leading to excision of O. Excision of O can be confirmed by qPCR. Additionally, the levels of viral DNA at different time points after excision can also be measured by qPCR. This experiment will illuminate the role of O in DNA synthesis throughout the lytic phase. One potential outcome would be that there is no DNA synthesis after the excision of O. Such a scenario would indicate that O is essential for continued DNA synthesis throughout the lytic phase. A second possible outcome is that there is no difference in the levels of DNA synthesis. Such a scenario would suggest that O, after the initiation of early rounds of DNA syntheses does not have a significant role in continued DNA synthesis throughout the lytic phase. Instead, an origin-independent mechanism mediates DNA synthesis, possibly involving recombinational events that provide a substrate for the initiation of DNA synthesis. A third possible outcome is that there is an intermediate level of viral DNA. Such a scenario would suggest that while the origin is necessary for continued DNA synthesis, it is not sufficient. This finding would suggest that there are multiple mechanisms by which DNA synthesis is initiated. 1) Origin-dependent DNA synthesis, and 2) Origin-independent DNA synthesis mediated by recombination.

Another finding of mine shows that the viral DNA amplification in individual cells lasts for approximately 13 hrs. What are the structures it adopts during this amplification

process? It is likely that the viral DNA replicon adopts theta structure early on [77], however, it isn't clear what structures it adopts subsequently. To analyze the structure of the whole viral DNA, total viral DNA can be isolated after cell cycle synchronization and visualized using electron microscopy (EM) [27]. In addition to giving us insights into viral DNA structures, EM will likely give us insights into the heterogeneity of the viral DNA as well, as suggested in a paper for HSV-1 DNA during its lytic phase [25] which however looked at asynchronous populations of cells. For EBV, these studies can be carried out using iD98HR1 cells. These cells support the lytic phase of EBV efficiently. After synchronization of iD98HR1 cells by the temperature variation method [76], subsequent induction of lytic phase and addition of EdC 30 min before the endpoint, intact DNA can be isolated at different stages of the lytic phase and viral DNA can be enriched using CsCl gradient. Viral DNA is denser the cellular DNA, therefore, CsCl gradient permits enrichment of viral DNA. EdC labeled DNA which will be dominantly viral can be further enriched using antibodies (also conjugated to biotin) against EdC. The viral DNA can then be visualized on an EM grid using streptavidin conjugated to gold metal. However, a potential difficulty is that viral DNA during the lytic phase is likely to be very big, much larger than viral DNA during latency [30], and therefore, the integrity of DNA may be compromised during DNA isolation. An independent approach that is likely to complement EM is the use of Single Molecules Analysis of Replicating DNA (SMARD)[78]. The viral DNA can be labeled using EdU/EdC and visualized after performing click chemistry which will render newly synthesized DNA fluorescent. The fluorescence microscopy techniques do not match the resolution of EM but will permit the analysis of DNA synthesis of large DNA molecules[79]. First, this technique permits

direct visualization of viral DNA molecules via EdU click chemistry (EdU is not incorporated into cellular DNA during the lytic phase). Second, it permits us to visualize the replication fork movement on the viral DNA. This visualization permits us to directly address the number of initiation sites on individual viral DNA molecules. There are two possible outcomes- 1) DNA synthesis initiation from one site- This would suggest that the DNA synthesis is initiating at a defined origin 2) DNA synthesis initiation from multiple sites- This would suggest that DNA synthesis is not dependent on individual origins but instead on multiple sites on a molecule. These observations will directly provide us with insights on the structure of viral DNA- Initiation from multiple sites would be consistent with recombination and branched structures.

The coating of cellular DNA by histones imparts stability to its structure by charge neutralization. However, viral DNAs amplified during the lytic phase do not have detectable histones[7]. So how are they charge-neutralized? There is no clear answer as to how the DNA is charge-neutralized.One study suggested the presence of positively charged polyamines in HSV-1 viral particles[80]. Previously, it has been established that polyamines, as organic cations interact with DNA[81]. I hypothesize that these organic cations charge neutralize viral DNA in the absence of detectable histones. To test this hypothesis, we will exploit a recently developed synthetic molecule conjugated to a TAMRA dye. This molecule can detect a variety of polyamines and can penetrate live cells [82]. These dyes can be used for intracellular imaging of polyamines. Therefore, the levels of polyamines in replication compartments can be directly visualized by imaging both replication compartments and polyamines and subsequently, quantifying the levels of polyamines in the replication compartments. If polyamines do neutralize viral DNA,

the increase in polyamines would be observed throughout the lytic phase as more viral DNA is synthesized. In addition, polyamines can be quantified in viral particles after they have been incubated with the dye. Subsequently, the solution can be washed, and the remaining particles quantified for fluorescence. Viral particles that do not encapsidate viral DNA serve as a negative control for the experiments. With these experiments one can begin to understand the role of polyamines in stabilizing viral DNA that lack histones. If polyamines are associated in replication compartments and viral particles, further analysis can be undertaken to detect individual polyamines such as spermine, spermidine and putrescine using traditional analytical chemistry [80].

During my graduate research, I have worked on factors that determine the viral DNA amplification process. The two question proposed above- One on how an origin plays a role in DNA amplification and second, how the amplified DNA is charge-neutralized to maintain its stability will directly build on my work here. More importantly, when the questions are addressed, the answers will provide fundamental insights into herpesvirology.

APPENDIX I.

DEVELOPMENT OF A METHOD TO CONTROL INTRACELLULAR LOCALIZATION OF PROTEINS

This work was done in collaboration with Dr.Aussie Suzuki and Alex Li. Dr. Suzuki is an assistant professor and Alex Li is an undergraduate at UW-Madison. I guided Alex Li in some of these experiments

Introduction

A part of the function of a protein depends on its location in a cell. Therefore, the ability to control the location of a protein in a cell will be a powerful technique to examine its function. In 2006, researchers developed the Auxin Inducible Degron (AID) system, a technique that allows rapid degradation (~26 min) [83] of a protein to understand the effect of a protein on cellular homeostasis. In this system, there are three key elements 1) Auxin (Au), 2) Auxin receptor (AID tag; IAA or IAA17 here onwards) and 3) Oryza sativa Transport Inhibitor Response 1 (OsTIR1). Auxin is a plant hormone that binds to the AID tag. OsTIR1 binds to Skp1 to form the Skp1-Cullin1-OsTIR1 complex (SCFTIR1) [84]. SCFTIR1 binds and ubiquitinates the AID tag bound to auxin and facilitates proteasome-dependent degradation of the AID-tag. In plants, this degradation of IAA eliminates its binding with Auxin Response Factors (ARFs) leading to transcriptional activation by ARFs. We are harnessing the biology of Au/IAA and ARFs evolved in plants to develop tools to control the intracellular localization of mammalian proteins to understand their function in cells. This technique once developed will provide the following advantages- 1) Toggling the location of protein that is present in multiple different compartments in a cell to a unique location such that we can understand the function of the protein in any intracellular compartment, 2) The proposed technique will be superior to the already existing AID system in that new proteins don't have to be re-synthesized, but instead, just have to be relocalized back to their original location by the removal of auxin. This new approach will eliminate the problem of re-expression of the protein as in the case of the original AID system which takes more time and could potentially be cell cycle-dependent and 3) In multiple

herpesviruses, it has been shown that both early viral RNAs and cellular RNAs are cleaved during the lytic phase. Therefore, the use of the already existing AID system will not enable re-expression of the proteins. However, our method which does not degrade the protein will be able to relocalize the protein efficiently to its original location. To summarize, this method will provide a toggle switch to localize a protein of choice to a unique location and relocalize the protein back to its original position rapidly, therefore, providing a facile way to study protein function at a defined cellular state.

Strategy

Three important components include 1) Auxin Response Factor 5(ARF5), 2) AID tag and 3) OsTIR1. IAA17 and ARF5 (from a pool of ARFs) were chosen because their interactions have been well characterized[85]. The protein of interest (POI) will be tagged with ARF5. Three different loci will be analyzed by fusing IAA17 to a nuclear export sequence (NES),a mitochondria localization sequence (MLS) or, a plasma membrane targeting sequence (PMTS). ARF5 and IAA17 have been shown to associatewith high affinity (Kd- 73nM). In the absence of Au, ARF5 will be bound to IAA17 and by default, will localize to the region where IAA17 is localized. In our example, it will localize to the cytoplasm (NES), to mitochondria (MLS) or the plasma membrane (PMTS). Therefore, the protein of interest will localize with IAA17. However, on the addition of Au, IAA17 will be degraded and the POI will relocalize to its bona fide location. The degradation of IAA17 will also require OsTIR1 to be expressed in cells.

RESULTS

Controlling intracellular protein location

To test our model, I generated plasmids that expressed PM/MLS/NES-IAA17-HA- P2A-mSc-ARF5 (Fig A1.1). This design ensured that mSc-ARF5 and IAA17 were expressed at approximately similar levels. Plasmids that only express IAA17 fused to targeting sequences were also generated. 293 cells were transfected with these plasmids. Subsequently, all the cells were visualized by live-cell microscopy and fixed-cell microscopy. IAA17 localized well to all sites- the cytoplasm, mitochondria, and the plasma membrane depending on the targeting sequence to which it was fused (Fig A1.1A). An increased localization of mSc-ARF5 to the plasma membrane was observed when IAA17 was fused to PM targeting sequence. Also, overexpression of IAA17 did not significantly increase the localization of mSc-ARF5 to IAA17. To ensure that the localization of mSc-ARF5 was specifically due to its interaction with IAA17, plasmids expressing PM/MLS/NES-IAA17-HA- P2A-mSc-ARF5(m) were generated. The ARF5 in this construct carries a mutation that significantly reduces ARF5's binding affinity to IAA17. If the localization of mSc-ARF5 was due to its interaction with IAA17, the mutation in ARF5 would abolish its localization with IAA17 to the targeted regions. As expected, mSc-ARF5 did not localize with IAA17.

Figure A1.1

A

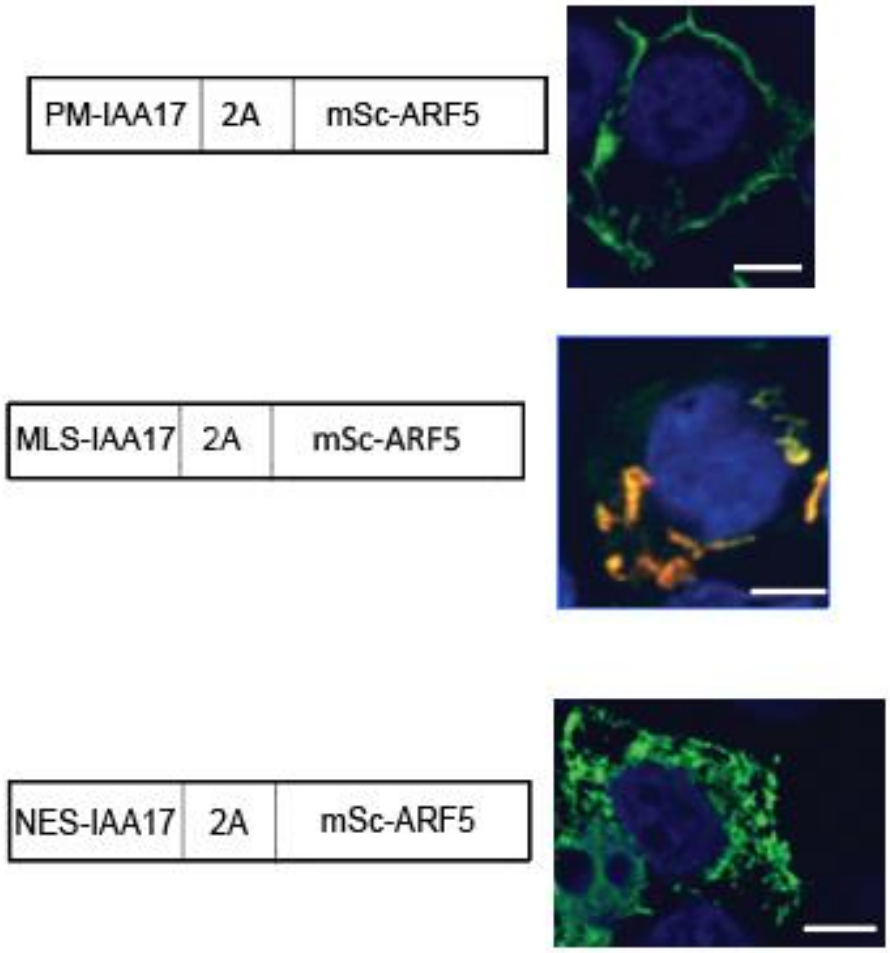

Fig A1.1 Targeting IAA17 to their respective intracellular locations A) Constructs encoding IAA17 with targeting sequence and mSc-ARF5. IAA17 localizes appropriately to a location depending on the targeting sequence to which it is fused. IAA17 is detected by immunofluorescence with antibodies against HA. Cellular DNA was stained using Dapi. Mitochondria were stained using MitoTracker (Invitrogen)

B

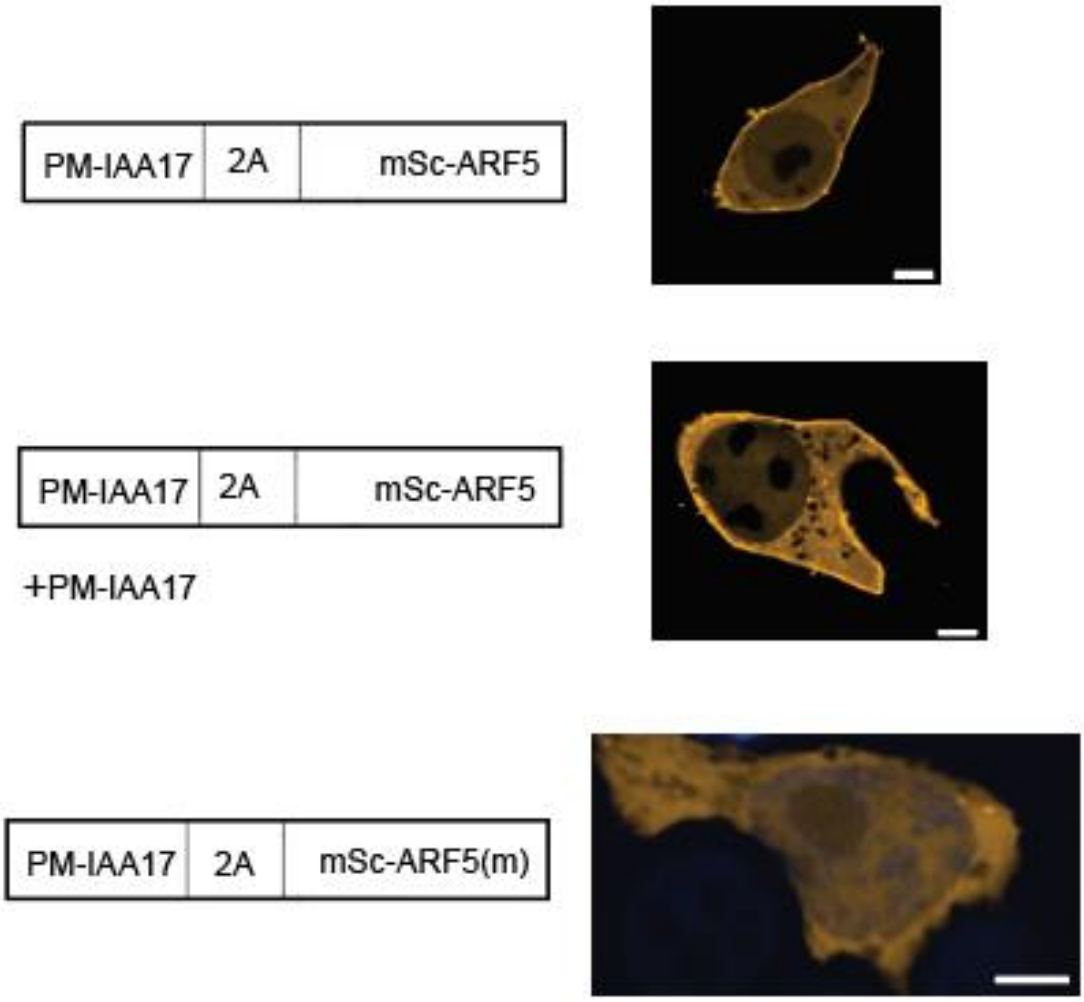

B) Localization of mSc-ARF5 when co-expressed with IAA17 fused to PM sequence. Bottom panel shows the expression of ARF5 when a mutation ARF5(m) reduces its interaction with IAA17. In both A&B, all cells in the imaging field (>20 cells) showed identical phenotype. Quantification of intensities is not available.

Future Directions

So far, I have shown that ARF5 can interact with IAA17 specifically to localize to the region to which IAA17 is targeted. The next set of experiments would entail analysis of ARF5 localization in the presence of Au in cells that express OsTIR1. To this end, 293 cells stably expressing OsTIR1 have been generated. The next step in the development of the method is to optimize the levels of IAA17 and ARF5 such that there is increased localization of ARF5 with IAA17. To obtain this goal, IAA17 and ARF5 will be stably expressed from cells such that IAA17 will be expressed at increasing levels to optimize the ratio of IAA17 to ARF5 to obtain increased ARF5 colocalization with IAA17. Once the optimal expression of IAA17 and ARF5 are obtained, ARF5 will be fused to BZLF1, a viral immediate early protein to control its location at different stages of the lytic phase. It is well known that BZLF1 is required for the initiation of DNA replication during EBV's early lytic phase. However, little is known about its function after the early stages of lytic phase. To address the uncertainty, this newly developed technique will be employed to monitor the function of BZLF1 at different stages of the lytic phase. Cells harboring EBV mutant lacking BZLF1 will be generated. Subsequently, IAA17-NES and BZLF1-ARF5 will be expressed in the cells. In the absence of Au, BZLF1 will be held in the cytoplasm. However, in the presence of Au, IAA 17 will be degraded, facilitating entry of BZLF1 into the nucleus of the cell. Initially, to initiate the DNA synthesis, Auxin will be added. However, to elucidate the role of BZLF1 after the initial round of DNA synthesis, the auxin will be washed away. This removal will relocalize BZLF1 back to the cytoplasm. The levels of viral DNA accumulated will be compared to cells in which auxin was not washed away. This experiment will allow us to determine if BZLF1

significantly contributes to DNA synthesis subsequent to the first round of DNA replication.

The experiments described will explore any role of oriLyt in viral DNA synthesis during EBV's lytic phase after the initial rounds of DNA synthesis. They constitute one approach to pursuing a "future direction" posed in Chapter 5.

APPENDIX II.

DEVELOPMENT OF A SAFE DERIVATIVE OF SARS-CoV-2

Introduction

SARS-CoV-2 is a novel strain of coronavirus that causes COVID19, a respiratory disease that can range from mild to severe illness and death. COVID19 has recently caused over 1 million deaths around the world and continues to cause fatalities across the globe. So far, there is no vaccine or an approved course of treatments for COVID19, other than remdesivir which only reduces symptoms. SARS-CoV-2 can be transmitted through several modes including contact, airborne droplets, fecal-oral and mother to child transmission. SARS-CoV-2 is a positive-sense RNA virus with an approximately 31 kb genome[86]. The RNA genome encodes viral proteins key to the virus overwhelming the host.

The spike protein S of SARS-CoV-2 binds to its human receptor ACE2 [87]. This binding mediates viral fusion to the cell membrane and its subsequent entry. The entry is also aided by the cell surface proteases TMPRSS2 or furin that proteolytically cleave S bound to ACE2 to facilitate entry of the virus[88]. Upon entry into the host cell, the viral RNA is released into the cytoplasm. This RNA which has a 5’ cap and 3’ poly A tail and supports translation of the viral RNA replication-transcription machinery (nsp 1-16) all of which are encoded by two ORFs, ORF 1a and ORF 1ab. The SARS-CoV-2 genome contains 14 open reading frames (ORFs), a 5’ UTR and a 3’UTR. The 5’UTR contains 7 stem loop structures and 3’ UTR contains one stem loop and a pseudoknot.

Figure A2.1

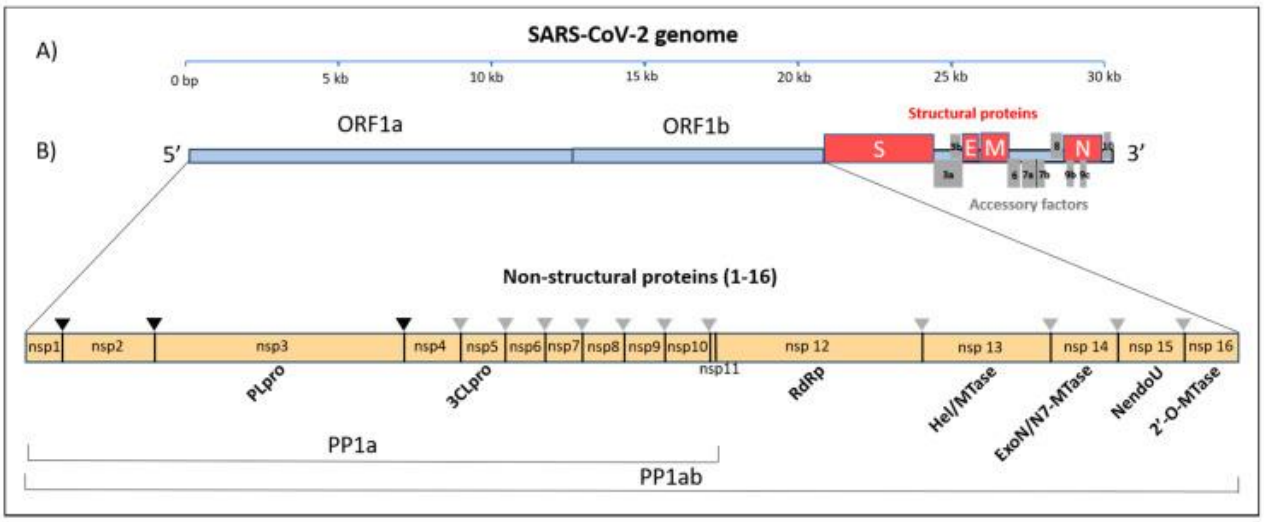

Fig A2.1 SARS-CoV-2 genome- The viral genome is ~31kb in length and encodes 16 non structural proteins (nsp) and four structural proteins. ORF 1a and ORF 1b (also known as ORF1ab) encode the nsp1-16 and is represented in blue and S,E,M and N are the structural proteins highlighted in red. This figure was adopted from [89]

These structures observed at the two ends of the genome are been known to influence transcription[90,91]. The viral RNA polymerase transcribes the positive sense RNA into negative sense. In addition to making a full length negative sense RNA, the replication machinery also synthesizes subgenomic RNAs (sgRNA) and this sgRNA synthesis requires transcriptional regulatory sequences (TRSs)[92]. The polymerase machinery pauses on arriving at a TRS. It can either continue to synthesis RNA into the adjacent gene or can pause transcription , translocate to the 5' end and continue the elongation

by copying the leader sequence. Such RNA synthesis is considered to be discountinuous. These sg RNAs and the full length viral RNA which have the anti leader sequence (sequence complementary to leader sequence) will serve as templates for mRNA transcription by viral transcriptases. These mRNAs then serve as templates for translation of structural proteins including – Membrane protein (M), Spike protein (S), Envelope protein (E),Nucleocapsid protein and also the non-structural proteins[92].The N protein specifically condenses with RNA sequences within the first 1000nt of the 5' end and phase separates, leading to the formation of ribonucleocapsids[93]. This process of encapsidation is dependent on structural elements, the length of viral RNA, temperature, and the concentration of N. While non-viral RNA can also be phase separated, it is not as efficient. The nucleocapsids then interact with other structural proteins, likely in the endoplasmic reticulum, and are packaged and moved to the ER-golgi intermediate compartment (ERGIC), after which the viral particle exits the cell via exocytosis[94].

The life-cycle of SARS-CoV-2 provides many opportunities for therapeutic intervention to inhibit the infection. One approved drug for treatment of COVID-19 is remdesivir, which is known to inhibit viral RNA polymerase. While remdesivir has been shown to be effective in reducing the viral load, it does not eliminate viral infection[95]. More recently, WHO has found that remdesivir is ineffective in many patients. In the trial, they found that remdesevir did not reduce the mortality, i.e., 2734 hospitalized patients either treated with remdesevir or a placebo yielded similar mortality rates of 11% and11.2% respectively. Therefore, there is an urgent need for an approved

vaccine. An ideal vaccine candidate would elicit broadly neutralizing antibodies (bNabs) without significant side effects often associated with therapeutic drugs.

Figure A2.2

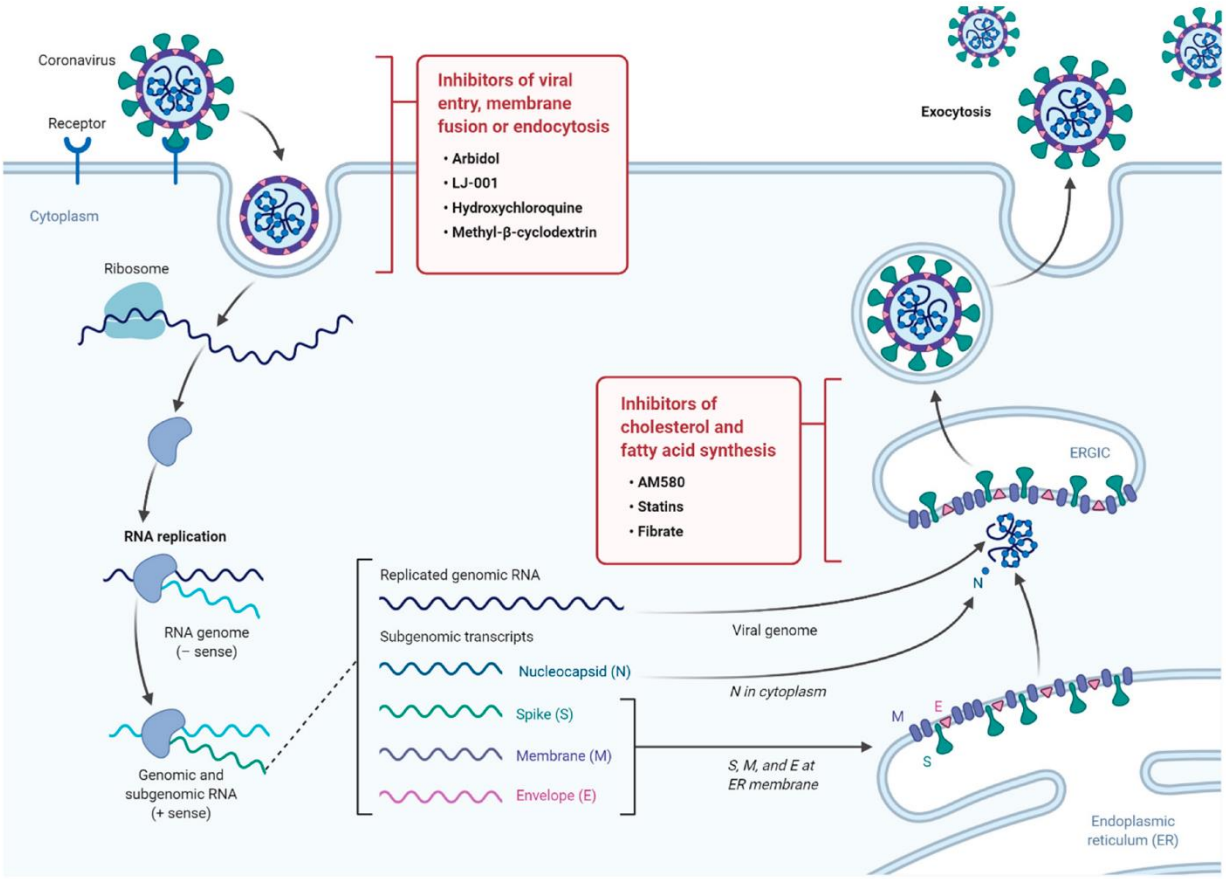

Fig A2.2 Life-cycle of SARS-CoV-2- The figure is a simplified overview of the infectious cycle of SARS-CoV-2 from the time of its entry to its exit from the host. The figure is adopted from [96]

In our lab, we are developing a multipurpose safe derivative of SARS-CoV-2 called CoV2-def which can be used variously- 1) To measure the ability of antibodies to efficiently neutralize the virus and prevent the entry cell entry of the virus, 2) To be a vaccine candidate and 3) To serve as a safe derivative that can be used in Biosafety Level 2 (BSL2) instead of BSL3 for researchers interested in the basic cell biology of SARS-CoV2.

Strategy

CoV2.def consists of the entire viral genome barring genes that encode two structural proteins E and M, but instead express EGFP and Nano-Luc or LNGFR. This modified genome can be replicated and transcribed but not packaged into a full-fledged viral particle. However, in cells that express E and M exogenously or conditionally, the viral genome can be successfully packaged into an infectious viral particle. On infecting a naïve cell (lacking E and M expression), these viral genomes can replicate but cannot be packaged, precluding their propagation. CoV-2 def will be developed such that producer cells can conditionally express the CoV2.def genome and package this infectious virus. Here are the sequential steps for the development of a system that conditionally expresses and packages CoV-2.def –

1) Development of 293 cells that express Tet-KRAB- Tet-KRAB is a fusion protein that binds to TetO sequences and blocks the expression of gene(s) downstream.

On addition of doxycycline, Tet-KRAB does not bind to TetO sequence anymore and this permits expression of downstream genes.

2) Conditional expression of M- M has been cloned into a retroviral plasmid that conditionally expresses M using the Tet-KRAB system.

Figure A2.3

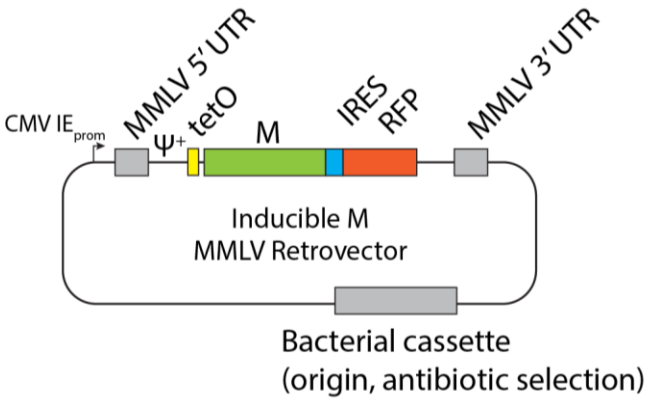

Fig A2.3 A pictorial representational of the plasmid that conditionally expresses M

3) Construction of CoV-2.def in an EBV derived plasmid- CoV-2.def will be cloned into an EBV-derived plasmid. The advantage of using an EBV-derived plasmid is that it can be maintained stably in mammalian cells and allow control of CoV-2.def expression. CoV-2.def will be assembled via Gibson assembly in two steps. First, ~2/3rd CoV-2.def (CoV2.def-part 1) will be assembled using Gibson Assembly. Once ~2/3rd is assembled, the remaining fragments will be cloned into 2/3rd CoV-2.def (CoV2.def-part 2) to generate the final plasmid, CoV-2.def.This plasmid

once generated, will be transfected, and maintained in the presence of selection (hygromycin) initially in a BSL3 lab.

Figure A2.4

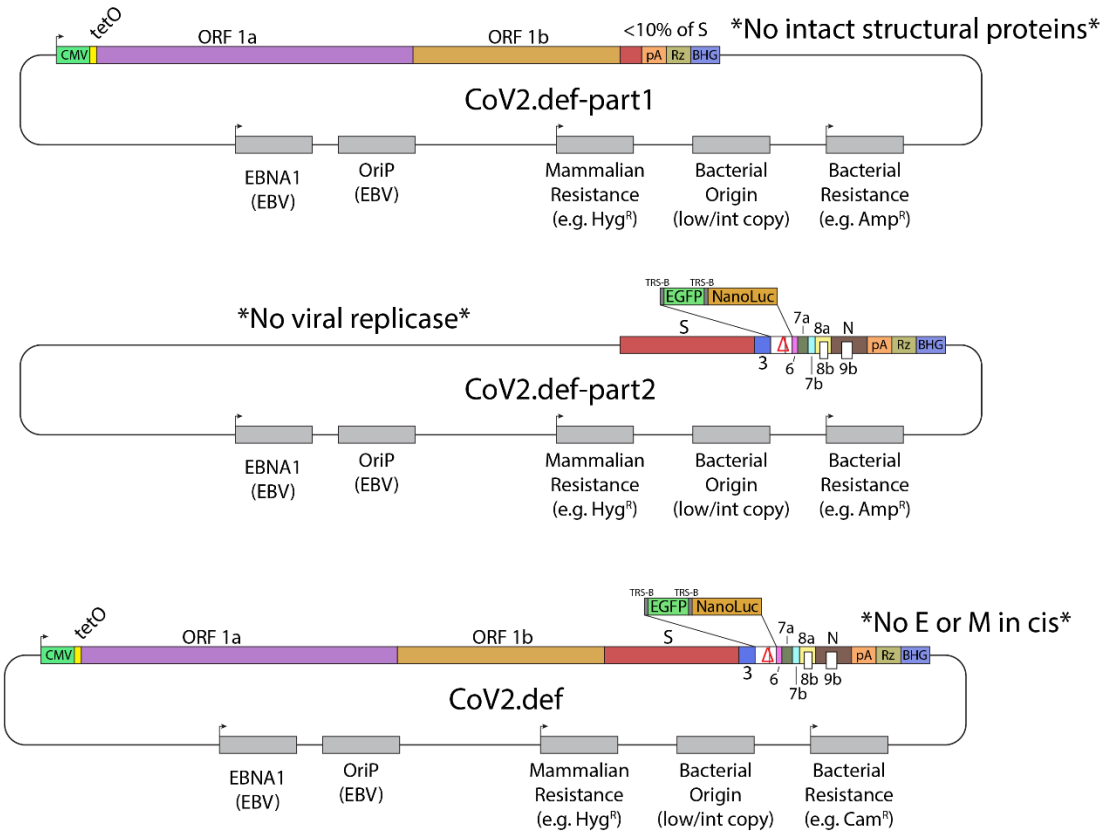

Fig A2.4- Pictorial representation of stepwise cloning of CoV2.def into EBV derived plasmid

4) Expression of E – The gene that encodes E will be cloned into a plasmid that includes a promoter that permits *in vitro* transcription, for example T7 promoter (Fig A2.5). Subsequently, E will be transcribed *in vitro,* and the RNA will be

transfected into 293 cells that harbor the CoV2.def and provirus that encodes inducibly expressed M.

Figure A2.5

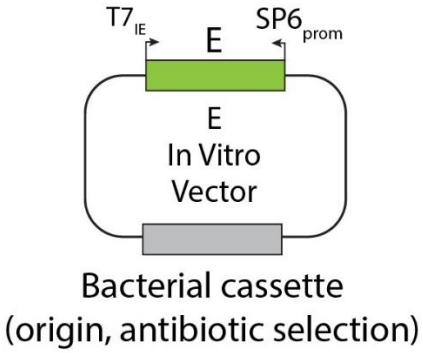

Fig A2.5 A pictorial representational of the plasmid that permits *in vitro* transcription of E

5) Post- transfection of E mRNA into cells that harbor CoV2.def and inducible M provirus, cells will be treated with doxycycline (10ng/ml). 48hrs later, the supernatant will be collected, and RT-qPCR will be carried out to measure the viral titers. In addition, the presence of M and E genes in the viral genomes will also be assayed to test for any potential recombination events. When we can establish that there is no recombination of CoV2.def, we can safely use CoV2.def in a BSL2 lab.

Results

Development of 293-Tet-KRAB cells – Retroviruses encoding Tet-KRAB were prepared. Subsequently, these retroviruses were used to infect 293 cells. Individual clones of cells were selected and assayed using FACS for the ability of cells to induce expression of genes downstream of TetO. We found that successful clones gave up to 1000-fold induction of genes on adding doxycycline.

Construction of CoV-2.def- The first part of constructing CoV-2.def was the assembly of 2/3rd CoV-2.def. We designed 10 fragments that make up 2/3rd CoV-2.def. These fragments were obtained as plasmids (pUC19 backbone). The fragments were amplified using PCR and were treated with *DpnI* overnight to remove the parental plasmids. Subsequently, we attempted to assemble all the 10 fragments using the Thermo Fisher Gene Art Gibson Assembly kit in one shot. After the Gibson assembly, the mix was transformed into DH10 bacteria and over 100 colonies were screened. However, none of them yielded a successful clone. Therefore, I switched to a Gibson assembly method aimed at assembling fragments 1-4, 5-7 and 8-10 separately.

Figure A2.6

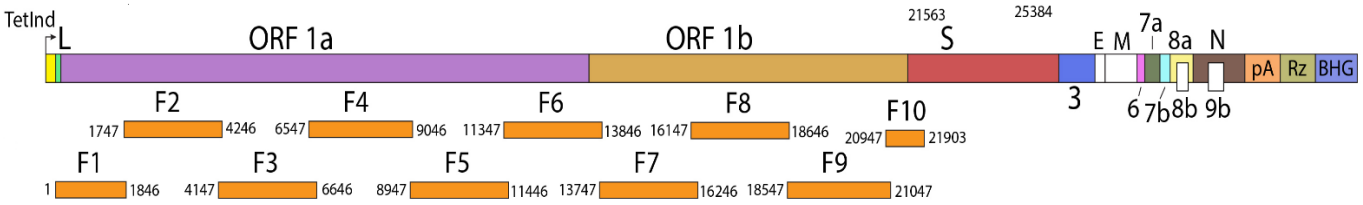

Figure A2.6- 2/3rd CoV-2.def and the Gibson Assembly fragments

We have now been able to assemble fragments 8-10 into the plasmid, PCR Blunt. Initially I screened 16 colonies using colony PCR for the presence of fragment 9. 12 out of 16 colonies showed presence of fragment 9. I then analyzed four of these colonies using restriction digest analysis with *BamHI* and *NotI*. All the clones showed the appropriate pattern for the presence of fragments 8-10. One of these clones were sequence verified. However, for the assembly of fragments 1-4 into PCR blunt, only 1 out of 148 colonies gave the correct pattern for colony PCR and restriction digest analysis. Subsequently, sequencing revealed two point mutations in this assembly that introduced stop codons. Currently, I am repairing these mutations using primers that have the correct sequence. In an attempt to assemble fragment 5-7, I screened 32 clones using colony PCR and restriction digest analysis. I found a major deletion in fragment 5 in 24 colonies and the other 8 colonies yielded only the parental plasmid. I am currently working on assembling fragment 5-7 in intermediate-copy and low-copy plasmids instead of PCR

blunt which is a high copy plasmid. In addition, I will also transform all the assemblies into a variety of bacterial strains, looking for hosts that limit the introduction of mutations.

To summarize, the Gibson assembly of CoV-2 fragments has been non trivial compared to other clonings I have done. Our current cloning results (both success and failures) indicate that CoV-2 fragments when expressed in bacteria are likely to be toxic and therefore, the results are likely to provide guidance on assembling viral fragments in the future which are similar in nature to CoV-2.

References

1. Sehrawat, S., Kumar, D. & Rouse, B. T. Herpesviruses: Harmonious pathogens but relevant cofactors in other diseases? *Frontiers in Cellular and Infection Microbiology* vol. 8 177 (2018).

2. Krishnan, H. H. *et al.* Concurrent Expression of Latent and a Limited Number of Lytic Genes with Immune Modulation and Antiapoptotic Function by Kaposi's Sarcoma-Associated Herpesvirus Early during Infection of Primary Endothelial and Fibroblast Cells and Subsequent Decline of Lytic Gene Expression. *J. Virol.* **78**, 3601–3620 (2004).

3. Sugden, B., Phelps, M. & Domoradzki, J. Epstein-Barr virus DNA is amplified in transformed lymphocytes. *J. Virol.* **31**, 590–595 (1979).

4. Sugden, B. Expression of Virus-Associated Functions in Cells Transformed in Vitro by Epstein-Barr Virus: Epstein-Barr Virus Cell Surface Antigen and Virus-Release from Transformed Cells. in *Immune Deficiency and Cancer* 165–177 (Springer New York, 1984). doi:10.1007/978-1-4684-4760-6_8.

5. Hammerschmidt, W. & Sugden, B. Replication of Epstein-Barr viral DNA. *Cold Spring Harb. Perspect. Biol.* **5**, (2013).

6. Dembowski, J. A., Dremel, S. E. & DeLuca, N. A. Replication-Coupled Recruitment of Viral and Cellular Factors to Herpes Simplex Virus Type 1 Replication Forks for the Maintenance and Expression of Viral Genomes. *PLOS Pathog.* **13**, e1006166 (2017).

7. Chiu, Y.-F., Sugden, A. U. & Sugden, B. Epstein-Barr viral productive amplification reprograms nuclear architecture, DNA replication, and histone deposition. *Cell Host Microbe* **14**, 607–18 (2013).

8. Nagaraju, T., Sugden, A. U. & Sugden, B. Four-dimensional analyses show that replication compartments are clonal factories in which Epstein–Barr viral DNA amplification is coordinated. *Proc. Natl. Acad. Sci.* (2019) doi:10.1073/PNAS.1913992116.

9. Djavadian, R., Chiu, Y.-F. & Johannsen, E. An Epstein-Barr Virus-Encoded Protein Complex Requires an Origin of Lytic Replication In Cis to Mediate Late Gene Transcription. *PLOS Pathog.* **12**, e1005718 (2016).

10. Hammerschmidt, W. & Sugden, B. Identification and characterization of oriLyt, a lytic origin of DNA replication of Epstein-Barr virus. *Cell* **55**, 427–33 (1988).

11. Lin, C. L. *et al.* Kaposi's Sarcoma-Associated Herpesvirus Lytic Origin (ori-Lyt)-Dependent DNA Replication: Identification of the ori-Lyt and Association of K8 bZip Protein with the Origin. *J. Virol.* **77**, 5578–5588 (2003).

12. Lin, C. L. *et al.* Kaposi's Sarcoma-Associated Herpesvirus Lytic Origin (ori-Lyt)-Dependent DNA Replication: Identification of the ori-Lyt and Association of K8

bZip Protein with the Origin. *J. Virol.* **77**, 5578–5588 (2003).

13. Schepers, A., Pich, D. & Hammerschmid, W. Activation of oriLyt, the lytic origin of DNA replication of Epstein-Barr virus, by BZLF1. *Virology* **220**, 367–376 (1996).

14. Baumann, M. *et al.* Activation of the Epstein-Barr Virus Transcription Factor BZLF1 by 12-O-Tetradecanoylphorbol-13-Acetate-Induced Phosphorylation. *J. Virol.* **72**, 8105–8114 (1998).

15. Rennekamp, A. J. & Lieberman, P. M. Initiation of Epstein-Barr virus lytic replication requires transcription and the formation of a stable RNA-DNA hybrid molecule at OriLyt. *J. Virol.* **85**, 2837–50 (2011).

16. Wang, Y. *et al.* Kaposi's Sarcoma-Associated Herpesvirus ori-Lyt-Dependent DNA Replication: cis-Acting Requirements for Replication and ori-Lyt-Associated RNA Transcription. *J. Virol.* **78**, 8615–8629 (2004).

17. Xu, Y., Cei, S. A., Rodriguez Huete, A., Colletti, K. S. & Pari, G. S. Human cytomegalovirus DNA replication requires transcriptional activation via an IE2- and UL84-responsive bidirectional promoter element within oriLyt. *J. Virol.* **78**, 11664–77 (2004).

18. Prichard, M. N. *et al.* Identification of Persistent RNA-DNA Hybrid Structures within the Origin of Replication of Human Cytomegalovirus. *J. Virol.* **72**, 6997–7004 (1998).

19. Watson, R. J., Sullivan, M. & Vande Woude', G. F. *Structures of Two Spliced Herpes Simplex Virus Type 1 Immediate-Early mRNA's Which Map at the Junctions of the Unique and Reiterated Regions of the Virus DNA S Component Downloaded from*. *JOURNAL OF VIROLOGY* http://jvi.asm.org/ (1981).

20. Jurak, I. *et al.* Numerous Conserved and Divergent MicroRNAs Expressed by Herpes Simplex Viruses 1 and 2. *J. Virol.* **84**, 4659–4672 (2010).

21. Weller, S. K. & Coen, D. M. Herpes simplex viruses: mechanisms of DNA replication. *Cold Spring Harb. Perspect. Biol.* **4**, a013011 (2012).

22. Sattler, C., Steer, B. & Adler, H. Multiple Lytic Origins of Replication Are Required for Optimal Gammaherpesvirus Fitness In Vitro and In Vivo. *PLOS Pathog.* **12**, e1005510 (2016).

23. Price, A. M. & Luftig, M. A. Dynamic epstein-barr virus gene expression on the path to B-cell transformation. in *Advances in Virus Research* vol. 88 279–313 (Academic Press Inc., 2014).

24. Strang, B. L. & Stow, N. D. Circularization of the Herpes Simplex Virus Type 1 Genome upon Lytic Infection. *J. Virol.* **79**, 12487–12494 (2005).

25. Jacob, R. J., Roizman, B. & Kovler, M. B. *Anatomy of Herpes Simplex Virus DNA VIII. Properties of the Replicating DNA*. *JOURNAL OF VIROLOGY* vol. 23 (1977).

26. Vlazny, D. A., Kwong, A. & Frenkel, N. Site-specific cleavage/packaging of herpes

simplex virus DNA and the selective maturation of nucleocapsids containing full-length viral DNA. *Proc. Natl. Acad. Sci. U. S. A.* **79**, 1423–1427 (1982).

27. Delius, H., Howe, C. & Kozinski, A. W. Structure of the replicating DNA from bacteriophage T4. *Proc. Natl. Acad. Sci. U. S. A.* **68**, 3049–3053 (1971).

28. Jacob, R. J., Morse, L. S. & Roizman, B. Anatomy of Herpes Simplex Virus DNA XII. Accumulation of Head-to-Tail Concatemers in Nuclei of Infected Cells and Their Role in the Generation of the Four Isomeric Arrangements of Viral DNA. *J. Virol.* **29**, 448–457 (1979).

29. Pfüller, R. & Hammerschmidt, W. Plasmid-like replicative intermediates of the Epstein-Barr virus lytic origin of DNA replication. *J. Virol.* **70**, 3423–31 (1996).

30. Bloss, T. A. & Sugden, B. Optimal lengths for DNAs encapsidated by Epstein-Barr virus. *J. Virol.* **68**, 8217–8222 (1994).

31. Severini, A., Scraba, D. G. & Tyrrell, D. L. Branched structures in the intracellular DNA of herpes simplex virus type 1. *J. Virol.* **70**, 3169–3175 (1996).

32. Schumacher, A. J. *et al.* The HSV-1 Exonuclease, UL12, Stimulates Recombination by a Single Strand Annealing Mechanism. *PLoS Pathog.* **8**, e1002862 (2012).

33. Weerasooriya, S., DiScipio, K. A., Darwish, A. S., Bai, P. & Weller, S. K. Herpes simplex virus 1 ICP8 mutant lacking annealing activity is deficient for viral DNA replication. *Proc. Natl. Acad. Sci. U. S. A.* **116**, 1033–1042 (2019).

34. Kops, A. de B. & Knipe, D. M. Formation of DNA replication structures in herpes virus-infected cells requires a viral DNA binding protein. *Cell* **55**, 857–868 (1988).

35. Chiu, Y. F. & Sugden, B. Epstein-Barr Virus: The Path from Latent to Productive Infection. *Annual Review of Virology* vol. 3 359–372 (2016).

36. Kobiler, O., Lipman, Y., Therkelsen, K., Daubechies, I. & Enquist, L. W. Herpesviruses carrying a Brainbow cassette reveal replication and expression of limited numbers of incoming genomes. *Nat. Commun.* **1**, 1–8 (2010).

37. Kobiler, O. *et al.* Herpesvirus Replication Compartments Originate with Single Incoming Viral Genomes. (2011) doi:10.1128/mBio.00278-11.

38. Chiu, Y. F., Sugden, A. U., Fox, K., Hayes, M. & Sugden, B. Kaposi's sarcoma-associated herpesvirus stably clusters its genomes across generations to maintain itself extrachromosomally. *J. Cell Biol.* **216**, 2745–2758 (2017).

39. Chang, L. *et al.* Herpesviral replication compartments move and coalesce at nuclear speckles to enhance export of viral late mRNA. *Proc. Natl. Acad. Sci. U. S. A.* **108**, E136-44 (2011).

40. Li, D., Fu, W. & Swaminathan, S. Continuous DNA replication is required for late gene transcription and maintenance of replication compartments in gammaherpesviruses. *PLOS Pathog.* **14**, e1007070 (2018).

41. Rowe, M. *et al.* Host shutoff during productive Epstein-Barr virus infection is mediated by BGLF5 and may contribute to immune evasion. *Proc. Natl. Acad. Sci. U. S. A.* **104**, 3366–3371 (2007).

42. Glaunsinger, B., Chavez, L. & Ganem, D. The Exonuclease and Host Shutoff Functions of the SOX Protein of Kaposi's Sarcoma-Associated Herpesvirus Are Genetically Separable. *J. Virol.* **79**, 7396–7401 (2005).

43. Vereide, D. T. & Sugden, B. Lymphomas differ in their dependence on Epstein-Barr virus. *Blood* **117**, 1977–85 (2011).

44. Salic, A. & Mitchison, T. J. A chemical method for fast and sensitive detection of DNA synthesis in vivo. *Proc. Natl. Acad. Sci. U. S. A.* **105**, 2415–2420 (2008).

45. Grady, L. M. *et al.* The exonuclease activity of HSV-1 UL12 is required for the production of viral DNA that can be packaged to produce infectious virus. *J. Virol.* **91**, e01380-17 (2017).

46. Chiu, Y.-F. *et al.* A comprehensive library of mutations of Epstein–Barr virus. *J. Gen. Virol.* **88**, 2463–2472 (2007).

47. Nanbo, A., Sugden, A. & Sugden, B. The coupling of synthesis and partitioning of EBV's plasmid replicon is revealed in live cells. *EMBO J.* **26**, 4252–62 (2007).

48. Hammerschmidt, W. & Sugden, B. Genetic analysis of immortalizing functions of Epstein–Barr virus in human B lymphocytes. *Nature* **340**, 393–397 (1989).

49. Takeda, D. Y. & Dutta, A. DNA replication and progression through S phase. *Oncogene* **24**, 2827–2843 (2005).

50. Pope, B. D. *et al.* Topologically associating domains are stable units of replication-timing regulation. *Nature* **515**, 402–405 (2014).

51. Zhao, Y., Shay, J. W. & Wright, W. E. Telomere terminal G/C strand synthesis: measuring telomerase action and C-rich fill-in. *Methods Mol. Biol.* **735**, 63–75 (2011).

52. Monier, K., Armas, J. C. G., Etteldorf, S., Ghazal, P. & Sullivan, K. F. Annexation of the interchromosomal space during viral infection. *Nat. Cell Biol.* **2**, 661–665 (2000).

53. Pombo, A., Ferreira, J., Bridge, E. & Carmo-Fonseca, M. Adenovirus replication and transcription sites are spatially separated in the nucleus of infected cells. *EMBO J.* **13**, 5075–5085 (1994).

54. Weitzman, M. D., Fisher, K. J. & Wilson, J. M. Recruitment of wild-type and recombinant adeno-associated virus into adenovirus replication centers. *J. Virol.* **70**, 1845–54 (1996).

55. Cziepluch, C. *et al.* H-1 parvovirus-associated replication bodies: a distinct virus-induced nuclear structure. *J. Virol.* **74**, 4807–15 (2000).

56. Prichard, M. N., Duke, G. M. & Mocarski, E. S. Human cytomegalovirus uracil

DNA glycosylase is required for the normal temporal regulation of both DNA synthesis and viral replication. *J. Virol.* **70**, 3018–25 (1996).

57. Bosse, J. B. *et al.* Remodeling nuclear architecture allows efficient transport of herpesvirus capsids by diffusion. *Proc. Natl. Acad. Sci.* **112**, E5725–E5733 (2015).

58. Hobbs, W. E. & DeLuca, N. A. Perturbation of cell cycle progression and cellular gene expression as a function of herpes simplex virus ICP0. *J. Virol.* **73**, 8245–55 (1999).

59. Church, G. A., Dasgupta, A. & Wilson, D. W. Herpes simplex virus DNA packaging without measurable DNA synthesis. *J. Virol.* **72**, 2745–51 (1998).

60. Hanson, L. K. *et al.* Murine Cytomegalovirus Capsid Assembly Is Dependent on US22 Family Gene M140 in Infected Macrophages. *J. Virol.* **83**, 7449–7456 (2009).

61. Granato, M. *et al.* Deletion of Epstein-Barr Virus BFLF2 Leads to Impaired Viral DNA Packaging and Primary Egress as Well as to the Production of Defective Viral Particles. *J. Virol.* **82**, 4042–4051 (2008).

62. Pavlova, S. *et al.* An Epstein-Barr virus mutant produces immunogenic defective particles devoid of viral DNA. *J. Virol.* **87**, 2011–22 (2013).

63. Kobiler, O., Brodersen, P., Taylor, M. P., Ludmir, E. B. & Enquist, L. W. Herpesvirus Replication Compartments Originate with Single Incoming Viral Genomes. *MBio* **2**, e00278-11 (2011).

64. Tomer, E. *et al.* Coalescing replication compartments provide the opportunity for recombination between coinfecting herpesviruses. *FASEB J.* **33**, 9388–9403 (2019).

65. Schmid, M., Speiseder, T., Dobner, T. & Gonzalez, R. A. DNA virus replication compartments. *J. Virol.* **88**, 1404–20 (2014).

66. Kulashreshtha, M., Mehta, I. S., Kumar, P. & Rao, B. J. Chromosome territory relocation during DNA repair requires nuclear myosin 1 recruitment to chromatin mediated by Y-H2AX signaling. *Nucleic Acids Res.* **44**, 8272–8291 (2016).

67. Toné, S. *et al.* Three distinct stages of apoptotic nuclear condensation revealed by time-lapse imaging, biochemical and electron microscopy analysis of cell-free apoptosis. *Exp. Cell Res.* **313**, 3635–3644 (2007).

68. Gargett, T. & Brown, M. P. The inducible caspase-9 suicide gene system as a ‘safety switch’ to limit on-target, off-tumor toxicities of chimeric antigen receptor T-cells. *Front. Pharmacol.* **5**, (2014).

69. Kudoh, A. *et al.* Epstein-Barr Virus Lytic Replication Elicits ATM Checkpoint Signal Transduction While Providing an S-phase-like Cellular Environment*. (2004) doi:10.1074/jbc.M411405200.

70. Inman, G. J., Binné, U. K., Parker, G. A., Farrell, P. J. & Allday, M. J. Activators of the Epstein-Barr Virus Lytic Program Concomitantly Induce Apoptosis, but Lytic Gene Expression Protects from Cell Death. *J. Virol.* **75**, 2400–2410 (2001).

71. Hollingworth, R., Horniblow, R. D., Forrest, C., Stewart, G. S. & Grand, R. J. Localization of Double-Strand Break Repair Proteins to Viral Replication Compartments following Lytic Reactivation of Kaposi's Sarcoma-Associated Herpesvirus. *J. Virol.* **91**, (2017).

72. Schaeffner, M. *et al.* BZLF1 interacts with chromatin remodelers promoting escape from latent infections with EBV. *Life Sci. Alliance* **2**, (2019).

73. Fajac, I. *et al.* Recombinant Escherichia coli as a gene delivery vector into airway epithelial cells. *J. Control. Release* **97**, 371–381 (2004).

74. Isberg, R. R. & Van Nhieu, G. T. The mechanism of phagocytic uptake promoted by invasin-integrin interaction. *Trends in Cell Biology* vol. 5 120–124 (1995).

75. Prichard, M. N., Duke, G. M. & Mocarski, E. S. *Human Cytomegalovirus Uracil DNA Glycosylase Is Required for the Normal Temporal Regulation of both DNA Synthesis and Viral Replication*. *JOURNAL OF VIROLOGY* vol. 70 http://jvi.asm.org/ (1996).

76. Ralph, M. *et al.* Promoting simultaneous onset of viral gene expression among cells infected with herpes simplex virus-1. *Front. Microbiol.* **8**, (2017).

77. Pfu¨ller, R. & Hammerschmidt, W. *Plasmid-Like Replicative Intermediates of the Epstein-Barr Virus Lytic Origin of DNA Replication*. *JOURNAL OF VIROLOGY* vol. 70 /pmc/articles/PMC190215/?report=abstract (1996).

78. Norio, P. & Schildkraut, C. L. Visualization of DNA replication on individual Epstein-Barr virus episomes. *Science (80-.).* **294**, 2361–2364 (2001).

79. Tourrière, H., Saksouk, J., Lengronne, A. & Pasero, P. Single-molecule Analysis of DNA Replication Dynamics in Budding Yeast and Human Cells by DNA Combing. *BIO-PROTOCOL* **7**, (2017).

80. Gibson, W. & Roizman, B. Compartmentalization of spermine and spermidine in the herpes simplex virion. *Proc. Natl. Acad. Sci. U. S. A.* **68**, 2818–2821 (1971).

81. van Dam, L., Korolev, N. & Nordenskiöld, L. Polyamine-nucleic acid interactions and the effects on structure in oriented DNA fibers. *Nucleic Acids Res.* **30**, 419–428 (2002).

82. Vong, K. K. H. *et al.* Cancer cell targeting driven by selective polyamine reactivity with glycine propargyl esters. *Chem. Commun.* **53**, 8403–8406 (2017).

83. Nishimura, K., Fukagawa, T., Takisawa, H., Kakimoto, T. & Kanemaki, M. An auxin-based degron system for the rapid depletion of proteins in nonplant cells. *Nat. Methods* **6**, 917–922 (2009).

84. Kanke, M. *et al.* Auxin-inducible protein depletion system in fission yeast. *BMC*

Cell Biol. **12**, 8 (2011).

85. Han, M. *et al.* Structural basis for the auxin-induced transcriptional regulation by Aux/IAA17. *Proc. Natl. Acad. Sci. U. S. A.* **111**, 18613–18618 (2014).

86. Kim, D. *et al.* The Architecture of SARS-CoV-2 Transcriptome. *Cell* **181**, 914-921.e10 (2020).

87. Yan, R. *et al.* Structural basis for the recognition of SARS-CoV-2 by full-length human ACE2. *Science (80-.).* **367**, 1444–1448 (2020).

88. Hoffmann, M. *et al.* SARS-CoV-2 Cell Entry Depends on ACE2 and TMPRSS2 and Is Blocked by a Clinically Proven Protease Inhibitor. *Cell* **181**, 271-280.e8 (2020).

89. Romano, M., Ruggiero, A., Squeglia, F., Maga, G. & Berisio, R. A Structural View of SARS-CoV-2 RNA Replication Machinery: RNA Synthesis, Proofreading and Final Capping. *Cells* vol. 9 1267 (2020).

90. Liu, P. & Leibowitz, J. RNA Higher-Order Structures Within the Coronavirus 5 0 and 3 0 Untranslated Regions and Their Roles in Viral Replication. *Mol. Biol. Sars-coronavirus* 47–61 (2009) doi:10.1007/978-3-642-03683-5_4.

91. Rangan, R. *et al.* RNA genome conservation and secondary structure in SARS-CoV-2 and SARS-related viruses: A first look. *RNA* **26**, 937–959 (2020).

92. Sola, I., Almazán, F., Zúñiga, S. & Enjuanes, L. Continuous and Discontinuous RNA Synthesis in Coronaviruses. *Annual Review of Virology* vol. 2 265–288 (2015).

93. Iserman, C. *et al.* Specific viral RNA drives the SARS CoV-2 nucleocapsid to phase separate Specific viral RNA drives the SARS-CoV-2 nucleocapsid to phase separate. doi:10.1101/2020.06.11.147199.

94. Fehr, A. R. & Perlman, S. Coronaviruses: An overview of their replication and pathogenesis. in *Coronaviruses: Methods and Protocols* vol. 1282 1–23 (Springer New York, 2015).

95. Beigel, J. H. *et al.* Remdesivir for the Treatment of Covid-19 — Preliminary Report. *N. Engl. J. Med.* (2020) doi:10.1056/nejmoa2007764.

96. Abu-Farha, M. *et al.* The role of lipid metabolism in COVID-19 virus infection and as a drug target. *International Journal of Molecular Sciences* vol. 21 3544 (2020).